

# The binding of NCAM to FGFR1 induces a specific cellular response mediated by receptor trafficking

Chiara Francavilla,<sup>1</sup> Paola Cattaneo,<sup>1</sup> Vladimir Berezin,<sup>2</sup> Elisabeth Bock,<sup>2</sup> Diletta Ami,<sup>1</sup> Ario de Marco,<sup>1</sup> Gerhard Christofori,<sup>3</sup> and Ugo Cavallaro<sup>1</sup>

<sup>1</sup>IFOM-FIRC Institute of Molecular Oncology, IFOM-IEO Campus, I-20139 Milano, Italy

<sup>2</sup>Protein Laboratory, Department of Neuroscience and Pharmacology, Panum Institute, University of Copenhagen, DK-2200 Copenhagen, Denmark

<sup>3</sup>Department of Biomedicine, Institute of Biochemistry and Genetics, University of Basel, CH-4058 Basel, Switzerland

**N**eural cell adhesion molecule (NCAM) associates with fibroblast growth factor (FGF) receptor-1 (FGFR1). However, the biological significance of this interaction remains largely elusive. In this study, we show that NCAM induces a specific, FGFR1-mediated cellular response that is remarkably different from that elicited by FGF-2. In contrast to FGF-induced degradation of endocytic FGFR1, NCAM promotes the stabilization of the receptor, which is recycled to the cell surface in a Rab11- and Src-dependent manner. In turn, FGFR1 recycling is required for NCAM-induced sustained activation of vari-

ous effectors. Furthermore, NCAM, but not FGF-2, promotes cell migration, and this response depends on FGFR1 recycling and sustained Src activation. Our results implicate NCAM as a nonconventional ligand for FGFR1 that exerts a peculiar control on the intracellular trafficking of the receptor, resulting in a specific cellular response. Besides introducing a further level of complexity in the regulation of FGFR1 function, our findings highlight the link of FGFR recycling with sustained signaling and cell migration and the critical role of these events in dictating the cellular response evoked by receptor activation.

## Introduction

FGF receptors (FGFRs) are cell surface receptor tyrosine kinases (RTKs) that, upon binding of FGFs, undergo dimerization and trans-phosphorylation (Beenken and Mohammadi, 2009), which generates multiple docking sites for several adaptor and effector proteins, thus resulting in the activation of various signaling pathways (Eswarakumar et al., 2005; Furdui et al., 2006). Typical effectors of FGFR activity are Shc and FGFR substrate-2 $\alpha$  (FRS-2 $\alpha$ ) that, by recruiting the Grb2–SOS complex, induce the activation of the Ras–Raf–Erk1/2 pathway (Eswarakumar et al., 2005). As for most RTKs, ligand binding induces FGFR internalization and Cbl-mediated ubiquitination followed by lysosomal degradation (Wong et al., 2002).

In addition to heparan sulfate proteoglycans (Yayon et al., 1991), FGF signaling can also be modulated by several membrane proteins (Polanska et al., 2009), including cell adhesion molecules (CAMs) of the cadherin and immunoglobulin (Ig-CAMs) superfamilies (Cavallaro and Christofori, 2004). Among the Ig-CAMs that functionally interact with FGFR,

the best characterized is neural CAM (NCAM), a cell surface glycoprotein whose extracellular portion contains five Ig-like domains and two FNIII (fibronectin type III) repeats (Hinsby et al., 2004). In the central nervous system, NCAM enhances intercellular adhesion, axonal growth, and neuronal migration through both homophilic NCAM-mediated cell–cell adhesion and heterophilic interactions with other membrane proteins or extracellular matrix components (Hinsby et al., 2004). After the pioneering work that implicated NCAM-mediated FGFR signaling in neurite outgrowth (Williams et al., 1994), the NCAM–FGFR association has been demonstrated in several cell types, including nonneural cells (Cavallaro et al., 2001; Kos and Chin, 2002; Sanchez-Heras et al., 2006; Francavilla et al., 2007). Recently, NCAM-derived peptides or protein domains have been reported to interact with FGFR1 and FGFR2 (Kiselyov et al., 2003; Christensen et al., 2006) and to modulate various FGFR-mediated neuronal functions (Hansen et al., 2008). Nevertheless, the biological significance

Correspondence to Ugo Cavallaro: ugo.cavallaro@ifom-ieo-campus.it

Abbreviations used in this paper: CAM, cell adhesion molecule; dn, dominant negative; EGFR, EGF receptor; FGFR, FGF receptor; NCAM, neural CAM; RTK, receptor tyrosine kinase; Tf, transferrin.

© 2009 Francavilla et al. This article is distributed under the terms of an Attribution–Noncommercial–Share Alike–No Mirror Sites license for the first six months after the publication date [see <http://www.jcb.org/misc/terms.shtml>]. After six months it is available under a Creative Commons License [Attribution–Noncommercial–Share Alike 3.0 Unported license, as described at <http://creativecommons.org/licenses/by-nc-sa/3.0/>].

of FGFR activation by NCAM has remained largely elusive, especially in nonneural cell types.

In this study, we have investigated the outcome of NCAM–FGFR interplay in fibroblasts and epithelial cells. To this goal, we used soluble versions of NCAM, which enabled us to perform a direct comparison with FGF, the classical FGFR ligand that acts as a soluble growth factor. Our data show that (a) NCAM is a novel, noncanonical ligand for FGFR1 and induces a specific set of FGFR-dependent biochemical events, leading to cell migration; (b) soluble NCAM stimulates FGFR1 signaling in the absence of cell surface NCAM; (c) NCAM induces the internalization of FGFR1 and, unlike FGF, promotes its recycling to the cell surface, resulting in sustained signaling; and (d) NCAM stimulates cell migration, and this effect requires FGFR1 recycling. These data provide novel insights into the regulation and function of FGFR.

## Results

### Soluble, NCAM-derived fragments mimic cell surface NCAM in activating FGFR

To gain insights into the functional outcome of the NCAM–FGFR interplay in nonneural cell types, we asked whether NCAM and FGFs, the classical FGFR ligands, elicit the same cellular response downstream of FGFR. We reasoned that, for a direct comparison with FGF, NCAM must be presented to FGFR as a soluble ligand rather than as a membrane protein. However, in most cases, NCAM occurs as a cell surface molecule, and therefore, we initially verified whether soluble NCAM-derived molecules recapitulated the FGFR-mediated function of membrane-associated NCAM.

First, by using the whole ectodomains of NCAM and FGFR1 in surface plasmon resonance and solid phase-binding assays (Fig. S1, A and B), we confirmed and extended previous data on the binding of recombinant or synthetic fragments of NCAM to FGFR1 and FGFR2 (Kiselyov et al., 2003; Christensen et al., 2006). We previously reported that the reconstitution of pancreatic  $\beta$ -tumor cells from NCAM knockout mice with full-length NCAM rescues both cell matrix adhesion and neurite outgrowth but only in the presence of an intact FGFR-mediated signaling, thus implicating an interplay between NCAM and FGFR (Cavallaro et al., 2001). The treatment of NCAM-deficient  $\beta$ -tumor cells with soluble NCAM-Fc, consisting of the extracellular portion of NCAM fused to the Fc fragment of IgG, rescued both cell matrix adhesion (Fig. S1 C) and neurite outgrowth (not depicted). In contrast, no effect was observed with an NCAM-Fc version deleted of the second FNIII repeat ( $\Delta$ FN2-Fc), which is where the FGFR-binding motif is located (Kiselyov et al., 2003). Very similar results were obtained on mouse fibroblast L cells, which express no endogenous NCAM (Cavallaro et al., 2001; Francavilla et al., 2007). On one hand, the forced expression of trans-membrane NCAM stimulated matrix adhesion of L cells, an effect that was abolished by the FGFR inhibitor PD173074 (Fig. S1 D). On the other hand, soluble NCAM-Fc promoted matrix adhesion of L cells via FGFR signaling, whereas  $\Delta$ FN2-Fc had no effect (Fig. S1 E). Thus, a soluble version of NCAM's ectodomain

was able to recapitulate the FGFR-dependent function of membrane-associated NCAM.

These observations validated NCAM-Fc as a suitable tool to study the impact of NCAM on FGFR function, and the physiological relevance of this approach is further supported by the notion that NCAM also occurs as a soluble protein naturally released by various cell types in vivo (Secher, 2008). However, the ectodomain of NCAM contains several modules that engage in both homophilic (i.e., NCAM–NCAM) and heterophilic interactions with various cell surface and extracellular matrix molecules (Nielsen et al., 2008). Thus, to focus specifically on the effect of NCAM binding to FGFR, the experiments with NCAM-Fc were complemented with the NCAM-derived FGL peptide, which mimics the binding to and activation of FGFR1 (Kiselyov et al., 2003). Indeed, both in cell matrix adhesion (Fig. S1 E) and in the assays described in the following paragraphs, we obtained convincing evidence that FGL recapitulates the FGFR-dependent function of NCAM-Fc.

### NCAM and FGF stimulate different FGFR1-mediated pathways

Membrane-associated NCAM inhibits FGF signaling in different cell types (Francavilla et al., 2007). Therefore, to compare the impact of NCAM on FGFR function with that of FGF, we selected the HeLa epithelial cell line, which does not express NCAM (Fig. S1 F). Furthermore, HeLa cells express all FGFR family members (Fig. 1 A) and are amenable to the biochemical and imaging approaches that were undertaken to this purpose. Finally, we verified that the ectopic expression of membrane-associated NCAM in HeLa cells did not affect the ability of soluble NCAM fragments to induce FGFR-mediated signaling (Fig. S1 F), further supporting the choice of this cell line as a model system suitable to investigating the effect of NCAM versus FGF.

When HeLa cells were treated for 10 min with FGF-2, NCAM-Fc, or FGL, each of these ligands stimulated the phosphorylation of FGFR1 to a similar extent (Fig. 1 A). In contrast, none of the ligands stimulated the phosphorylation of FGFR2 or FGFR3, suggesting that NCAM, similar to FGF-2 (Itoh and Ornitz, 2004), does not activate the epithelial isoforms of these FGFR family members. FGFR4 underwent phosphorylation in response to FGF-2, but not to FGL or NCAM-Fc, thus indicating that NCAM-derived ligands selectively induced the activation of FGFR1. The stimulation of HeLa cells with FGF-2, FGL, or NCAM-Fc led to the activation of FRS-2 $\alpha$  and PLC- $\gamma$ , two classical FGFR substrates (Eswarakumar et al., 2005), which is an effect abolished by PD173074 (Fig. 1 B). FGF-2 induced the phosphorylation of Shc adaptor proteins, whereas no effect was observed with either NCAM-Fc or FGL (Fig. 1 B). Non-RTKs of the Src family have been implicated in NCAM signaling (Williams et al., 1994; Kiryushko et al., 2006), and, indeed, the treatment of HeLa cells with NCAM-Fc or FGL but not with FGF-2 induced FGFR-dependent Src activation (Fig. 1 B). However, FGF-2 did induce Src phosphorylation in NIH-3T3 cells (unpublished data), thus pointing to cell type-specific activities of this growth factor (Dailey et al., 2005). Finally, the activation of Erk1/2 was induced by FGF-2, NCAM-Fc, and

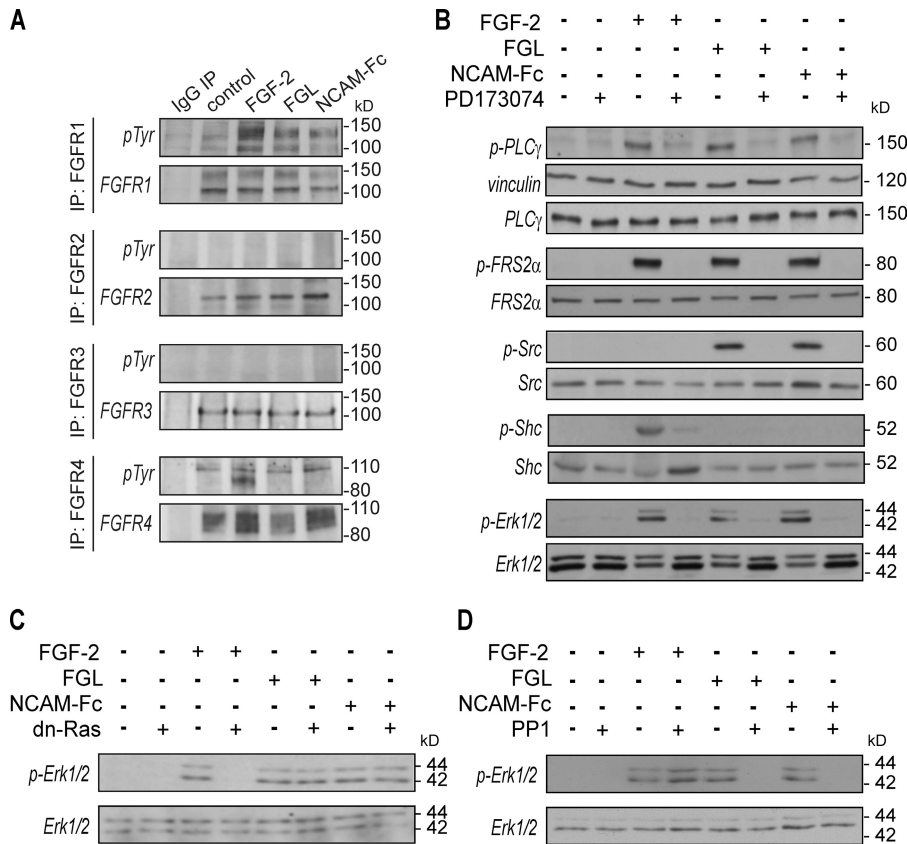


**Figure 1. NCAM and FGF activate distinct FGFR-mediated signaling pathways.** (A) Cell lysates (5 mg) from HeLa cells stimulated for 10 min with FGF-2, FGL, or NCAM-Fc were immunoprecipitated (IP) with control IgG or antibodies against individual FGFR types (FGFR1–4) and immunoblotted for phosphotyrosine (top) and for the corresponding FGFR types (bottom). (B, top) Equal loading for phospho-PLC- $\gamma$  was verified by immunoblotting for vinculin. (B–D) HeLa cells were stimulated for 10 min with FGF-2, FGL, or NCAM-Fc with or without a pretreatment with PD173074 (B) or PP1 (D). (C) Cells were transfected with dn-Ras or an empty vector before the stimulation (see Fig. S2 B for the expression of dn-Ras). Cell lysates were immunoblotted for phospho-PLC- $\gamma$ , phospho-FRS-2 $\alpha$ , phospho-Shc, phospho-Src, and phospho-Erk1/2 followed by immunoblotting for total PLC- $\gamma$ , FRS-2 $\alpha$ , Shc, Src, and Erk1/2 as indicated.

FGL in an FGFR-dependent manner, as demonstrated by the use of PD173074 (Fig. 1 B) or by the cell transfection with dominant-negative (dn) FGFR1 (Fig. S2 A). However, the underlying mechanisms were different because FGF-induced activation of Erk1/2 was mediated by Ras, which instead was not involved downstream of NCAM-derived ligands (Fig. 1 C). Rather, the phosphorylation of Erk1/2 stimulated by NCAM-Fc and FGL required Src signaling because it was abolished by two distinct Src inhibitors, PP1 (Fig. 1 D) and SU6656 (Fig. S2 C), as well as by the forced expression of dn-Src (Fig. S2 D). In contrast, Src inhibition did not affect FGF-2-induced Erk1/2 activation (Fig. 1 D; and Fig. S2, C and D). The dichotomy between NCAM and FGF signaling was also confirmed in L cells (Fig. S2, E–H), implying that it is not restricted to a single-cell type. Overall, these findings indicated that NCAM acts as a noncanonical ligand for FGFR in different cell types and induces a set of FGFR-dependent signaling events distinct from that elicited by FGF.

### NCAM induces sustained activation of FGFR effectors

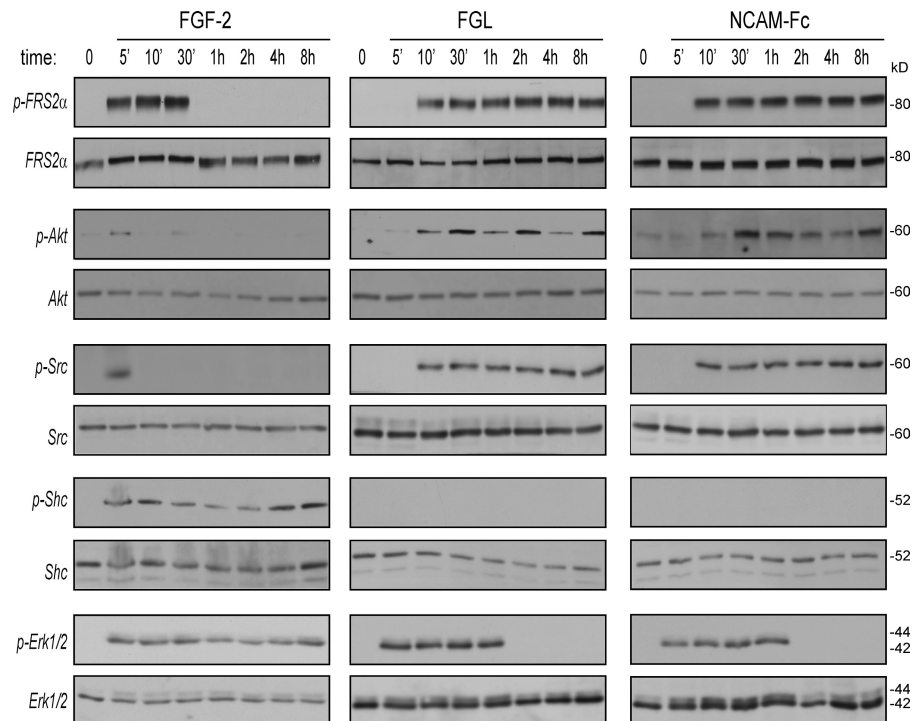
We investigated the kinetics of FGFR signaling upon stimulation of HeLa cells with FGF-2, NCAM-Fc, or FGL for different time periods. As shown in Fig. 2 (left), FGF-2 induced a transient activation of FRS-2 $\alpha$  that declined after 30 min. Weak phosphorylation of Akt, another classical FGFR effector (Eswarakumar et al., 2005), was observed at 5 min but became undetectable at later time points. Immunoblotting for phospho-Src showed a very weak band after 5 min of FGF-2 stimulation,

which was no longer detectable after longer treatments, confirming and extending the data shown in Fig. 1 A. A prolonged phosphorylation was instead observed for Shc and Erk1/2 (Fig. 2, left). In contrast to FGF-2, both FGL (Fig. 2, middle) and NCAM-Fc (Fig. 2, right) induced sustained phosphorylation of FRS-2 $\alpha$ , Akt, and Src, whereas no phosphorylation of Shc was detected. Instead, Erk1/2 activation occurred in a transient manner, declining after 1 h of treatment (Fig. 2, middle and right). Therefore, the interaction of NCAM or FGF with FGFR induced the activation of signaling cascades with remarkably different kinetics, with NCAM stimulating the sustained activation of the FGFR effectors FRS-2 $\alpha$ , Src, and Akt and transient activation of Erk1/2.

### FGFR1 is stabilized and recycled to the cell surface upon NCAM stimulation

To verify whether the sustained activation of FGFR effectors upon NCAM-mediated stimulation depended on the intracellular fate of FGFR1, we used imaging technologies. Because HeLa cells express only a modest amount of endogenous FGFR1, we transfected them with HA-tagged FGFR1. In agreement with previous data (Zhang et al., 2001), ectopically expressed HA-FGFR1 was not constitutively active and was responsive to FGF or NCAM stimulation (unpublished data). We applied an immunofluorescence-based method that allowed us to monitor receptor internalization, degradation, and recycling (see Materials and methods). In cells treated with FGF-2, NCAM-Fc, or FGL for  $\leq 60$  min, HA-FGFR1 gradually disappeared from the cell surface (Fig. 3 A, left) and accumulated in the cytosol (Fig. 3 A,

**Figure 2. NCAM induces sustained signaling.** Lysates from HeLa cells stimulated for the indicated time intervals with FGF-2 (left), FGL (middle), or NCAM-Fc (right) were immunoblotted for phospho-FRS-2 $\alpha$ , phospho-Akt, phospho-Src, phospho-Shc, or phospho-Erk1/2 followed by immunoblotting for total FRS-2 $\alpha$ , Akt, Src, Shc, or total Erk1/2 as indicated.



right). At 30 min, both surface and cytosolic staining for HA-FGFR1 were observed, suggesting that the receptor was not completely internalized at this time point. Instead, HA-FGFR1 was mostly detected in the cytosol upon 60-min stimulation (Fig. 3 A, right). These results were further validated by biochemical assays aimed at measuring the internalization of endogenously expressed FGFR1, an approach that revealed a comparable internalization rate between FGF-2 and FGL (Fig. S3 A). Therefore, the difference in the duration of FGFR1 signaling downstream of NCAM versus FGF is not the result of different kinetics of receptor endocytosis. Several RTKs, after ligand-induced internalization, enter the degradative pathway, a key mechanism underlying signal attenuation (Dikic and Giordano, 2003). To verify whether endogenous FGFR1 was degraded upon FGF versus NCAM stimulation, HeLa cells were treated with FGF-2, NCAM-Fc, or FGL for increasing time periods. The treatment was performed in the presence of cycloheximide to minimize the contribution of newly synthesized FGFR1. In agreement with previous observations (Haugsten et al., 2005), nearly complete loss of FGFR1 was observed between 1 and 2 h of FGF stimulation. In contrast, cells stimulated with FGL or NCAM-Fc exhibited remarkable levels of FGFR1 at all time points, with the receptor remaining well detectable even after 8 h of treatment (Fig. 3 B). As a possible mechanism accounting for NCAM-dependent stabilization of FGFR1, we verified whether NCAM and FGF exert a differential control on the degradation of the receptor. Because FGFR1 degradation is driven by Cbl-mediated ubiquitination (Wong et al., 2002), we investigated this pathway in HA-FGFR1-transfected HeLa cells. Our results revealed that, in sharp contrast to FGF-2, FGL did not induce HA-FGFR1 ubiquitination (Fig. 4 A). The association of Cbl with FRS-2 $\alpha$  is a prerequisite for FGF-induced ubiquitination of FGFR1 (Wong et al., 2002), and indeed, we

readily detected the Cbl-FRS-2 $\alpha$  complex in FGF-2-stimulated HeLa cells. Instead, cell treatment with FGL did not induce any association between Cbl and FRS-2 $\alpha$  (Fig. 4 B). Thus, unlike FGF-2, NCAM stimulation of FGFR1 does not result in Cbl-mediated receptor ubiquitination, likely accounting for the stabilization of the receptor itself.

A clear indication of the cellular fate of stabilized FGFR1 came from the immunofluorescence analysis of HA-FGFR1-transfected HeLa cells (Fig. 3 A). At 2 and 4 h, neither surface nor cytosolic HA-FGFR1 was detected in FGF-2-treated cells, which is consistent with FGF-induced degradation of FGFR. In contrast, massive recycling of HA-FGFR1 to the cell surface occurred in cells stimulated with FGL or NCAM-Fc (Fig. 3 A, left). The quantification of the immunofluorescence results confirmed that both NCAM and FGF-2 promote the internalization of FGFR1 (Fig. S3 B, middle), but receptor recycling is only observed upon NCAM stimulation (Fig. S3 B, bottom). The dramatic decrease in overall HA-FGFR1 signal in FGF-2-treated cells (Fig. S3 B, top) is consistent with receptor degradation. We also used a modified version of the biochemical method used for the internalization assay (see Materials and methods) to investigate the fate of endogenous FGFR1 after cell stimulation. This technique confirmed that NCAM stimulation results in FGFR1 stabilization and recycling to the cell surface as opposed to FGF-induced degradation of the receptor (Fig. 3 C). The apparent delay in FGFR1 degradation observed in immunofluorescence-based as compared with biochemical assays is likely caused by the antibody prebound to FGFR1 (see Materials and methods). Indeed, when we performed the biochemical assay in the presence of the antibody, both FGF-induced degradation and FGL-dependent recycling of FGFR1 were delayed (Fig. S3 C). The differential fate of internalized FGFR1 upon stimulation with FGF versus NCAM was further confirmed by

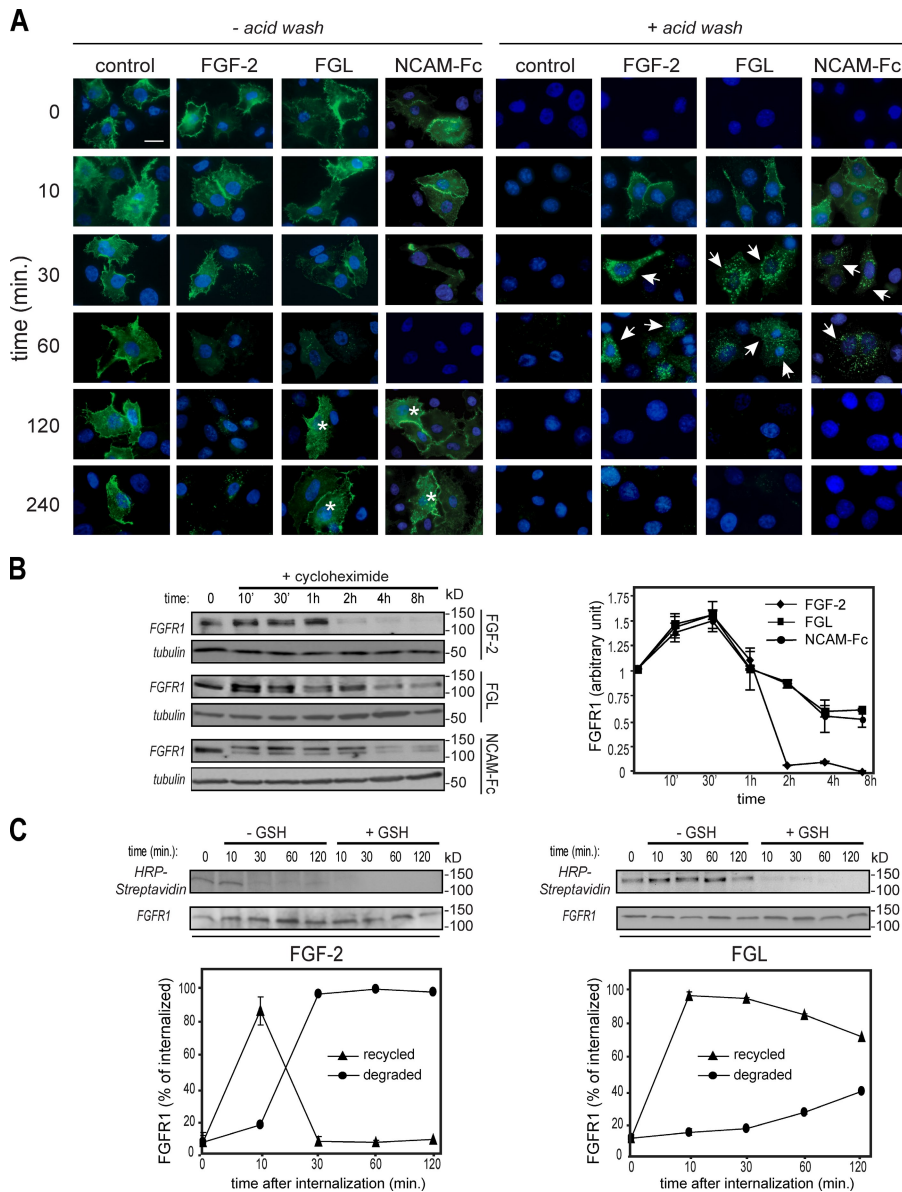


**Figure 3. FGFR1 is recycled to the cell surface upon NCAM stimulation.** (A) The internalization (+acid wash) and recycling (–acid wash) of HA-FGFR1 (green) in transfected HeLa cells stimulated with FGF-2, FGL, or NCAM-Fc were monitored as described in Materials and methods. Arrows indicate cells with internalized HA-FGFR1. Asterisks indicate cells where HA-FGFR1 recycled back to the cell surface. Bar, 10  $\mu$ m. (B, left) Lysates from HeLa cells stimulated with FGF-2, FGL, or NCAM-Fc for the indicated time intervals in the presence of cycloheximide were immunoblotted for FGFR1 using tubulin as loading control. The presence of a doublet in lysates from cycloheximide-treated cells might reflect the accumulation of an immature FGFR1 form as a consequence of the protein synthesis block. (right) Densitometric quantitation of FGFR1 in cells stimulated as described for the left panel. Data refer to the ratio between FGFR1 and tubulin for each time point. (C) Surface-biotinylated HeLa cells were stimulated with FGF-2 (left) or FGL (right). The rate of FGFR1 degradation and recycling (expressed as a percentage of internalized receptor) was determined as described in Materials and methods. The blots show the results of a representative experiment. Graphs show the means  $\pm$  SD from three independent experiments.

colocalization studies using EEA1 (Mu et al., 1995), LAMP-2 (Chen et al., 1985), and transferrin (Tf; Hopkins, 1983) as markers of early endosomes, lysosomes, and recycling vesicles, respectively. After a 10-min stimulation with either FGF-2 or NCAM-derived ligands, HA-FGFR1 was localized in early endosomes (Fig. 5 A), thus confirming that both FGF and NCAM promote FGFR endocytosis. Cell stimulation for 60 min with FGF-2, but not FGL or NCAM-Fc, resulted in HA-FGFR1 accumulation in lysosomes (Fig. 5 B), thus supporting the notion that FGF promotes lysosome-mediated degradation of FGFR1 (Haugsten et al., 2005), as also confirmed by our immunoblotting analysis (Fig. S3 D, left). Along this line, the lysosome inhibitor chloroquine induced the cytosolic accumulation of FGF-activated FGFR1 (Fig. S3 D, right). In contrast, in cells stimulated with FGL or NCAM-Fc, but not with FGF-2, HA-FGFR1 entered the recycling compartment (Fig. 5 C). We further investigated the recycling of HA-FGFR1 by analyzing its colocalization with Rab11, a small GTPase involved in receptor

recycling (Jones et al., 2006). In cells stimulated with FGL or NCAM-Fc, HA-FGFR1 showed extensive colocalization with Rab11, whereas no costaining was observed in FGF-2–treated cells (Fig. 5 D).

Collectively, these results indicate that FGFR1 enters early endosomes upon both FGF-2 and NCAM stimulation but is then sorted to divergent routes. In FGF-2–stimulated cells, FGFR1 is targeted for lysosomal degradation, whereas NCAM promotes the stabilization of FGFR1 followed by its recycling to the cell surface via Rab11-positive vesicles.

As a possible mechanism accounting for FGFR1 recycling in NCAM-stimulated cells, we focused on Src activity based on the considerations that (a) sustained Src activation was an NCAM-specific effect (Figs. 1 and 2) and that (b) Src has been implicated in the trafficking of FGFR1 (Sandilands et al., 2007). Thus, HA-FGFR1–transfected HeLa cells were pretreated with either PPI or SU6656 before monitor receptor trafficking in FGF-2– or NCAM-stimulated cells. Receptor recycling was

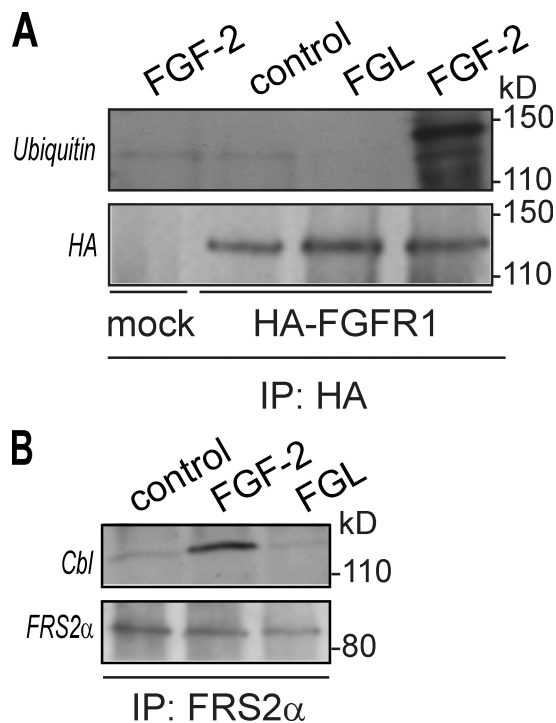


**Figure 4. Differential effect of NCAM and FGF on Cbl-mediated ubiquitination of FGFR1 and the association of Cbl with FRS-2 $\alpha$ .** (A) Lysates (3 mg) from HA-FGFR1-transfected HeLa cells stimulated for 10 min with FGF-2 or FGL were immunoprecipitated (IP) with anti-HA and immunoblotted for ubiquitin (top) followed by immunoblotting for HA (bottom). Mock-transfected cells stimulated with FGF-2 were used as negative control. (B) Lysates (1 mg) from HeLa cells stimulated for 10 min with FGF-2 or FGL were immunoprecipitated with antibodies against FRS-2 $\alpha$  and immunoblotted for Cbl (top) followed by immunoblotting for FRS-2 $\alpha$  (bottom).

no longer observed in NCAM-stimulated cells that were preincubated with Src inhibitors (Fig. 6 A), and the lack of either cell surface or cytosolic staining for HA-FGFR1 pointed to receptor degradation. Because these findings implicate Src in NCAM-dependent stabilization of FGFR1, we determined the effect of inhibiting Src on the recruitment of Cbl to FRS-2 $\alpha$  upon FGFR stimulation with FGF-2 versus FGL. Intriguingly, in PP1- or SU6656-treated cells, Cbl formed a complex with FRS-2 $\alpha$  even upon FGL stimulation (Fig. 6 B). This resulted in FGL promoting FGFR1 ubiquitination to a level comparable with FGF-2 (Fig. S4 A). Thus, the stabilization and recycling of FGFR observed upon NCAM stimulation implicates an active role of Src in preventing the association of Cbl with FRS-2 $\alpha$  and the consequent ubiquitination of FGFR1.

#### NCAM stimulates cell migration, which requires FGFR1 recycling

The dichotomy in FGFR signaling and trafficking induced by NCAM versus FGF raised the possibility that the two ligands elicit different FGFR-mediated cellular responses. To verify this hypothesis, we focused on cell migration and proliferation, two processes linked with FGFR function (Boilly et al., 2000). Monolayer-wounding assays combined with time-lapse video microscopy revealed that both FGL and NCAM-Fc promoted the migration of HeLa cells, whereas FGF-2 did not (Fig. 7,

A and B; and Videos 1–4). Both the covered distance and the speed of migrating cells were enhanced by NCAM-derived ligands (Fig. 7, A and B). Similar results were obtained with a 3D assay for cell migration based on modified Boyden chambers, with FGL and NCAM-Fc inducing the migration of HeLa (Fig. 7 C) and L cells (Fig. S4 B and not depicted), whereas FGF-2 failed to do so. In contrast,  $\Delta$ FN2-Fc did not promote cell migration (Fig. 7 C), supporting the key role of NCAM interaction with FGFR. Along the same line, NCAM-induced cell migration was abolished by either a pretreatment of cells with PD173074 (Fig. 7 C) or by the transfection with dn-FGFR1 (Fig. 7 D). The compound AG1478, a chemical inhibitor of EGF receptor (EGFR), showed no effect on FGL-induced cell migration, whereas it blocked the migration of EGF-stimulated cells (Fig. S4 D), thus supporting the specificity of the NCAM interaction with FGFR. Moreover, PP1, SU6656, dn-Src, and PD98059 repressed NCAM-induced cell migration (Fig. 7 C and Fig. S4 E), which indicated the requirement for both Src and Erk1/2 activity.

In agreement with our previous results (Francavilla et al., 2007), FGF-2 exerted a strong proliferative effect on both HeLa and L cells. In contrast, FGL had no impact on cell proliferation (Fig. 7 F and Fig. S4 C), confirming previous observations with NCAM-Fc (Francavilla et al., 2007). Thus, NCAM and FGF elicit distinct, FGFR-mediated cellular responses in both epithelial cells and fibroblasts, with NCAM promoting cell migration and FGF inducing cell proliferation.

Based on the promigratory activity of NCAM and on the stabilization (and thus recycling) of FGFR1, we verified whether NCAM-induced migration requires its ability to promote FGFR1 recycling. To this goal, HeLa cells were transfected with dn-Rab11, which blocks the recycling pathway (Ren et al., 1998). Indeed, HA-FGFR1 recycling was no longer observed in NCAM-stimulated HeLa cells transfected with dn-Rab11, whereas it was not affected in cells expressing wild-type Rab11 (Fig. 8 A). In agreement with this, dn-Rab11 caused the retention of internalized HA-FGFR1 in early endosomes (Fig. S5 A). To confirm the role of Rab11 in FGFR1 recycling, the expression of the three members of the Rab11 subfamily, namely Rab11a, Rab11b, and Rab25 (Prekeris, 2003), was ablated by using the RNAi technology. Similar to dn-Rab11, the knockdown of Rab11 genes resulted in the block of HA-FGFR1 recycling in FGL-stimulated cells (Fig. 8 B). Thus, we used both the ectopic expression of dn-Rab11 and the knockdown of endogenous Rab11 genes to investigate the contribution of Rab11 GTPases to NCAM-FGFR-dependent cell migration. Although dn-Rab11 abrogated the migratory response of HeLa cells to FGL (Fig. 8 C, left), it failed to inhibit cell migration in response to EGF, which is consistent with previous results (Palmieri et al., 2006). Analogous results were obtained when Rab11 expression was reduced by siRNA (Fig. 8 C, right). Thus, the recycling of FGFR1 via Rab11-dependent pathway is a specific prerequisite for NCAM-stimulated cell migration. In addition, the inactivation of endogenous Rab11 with either dn-Rab11 or siRNA-mediated knockdown caused the loss of sustained Src activation in response to NCAM stimulation, whereas no effect was observed on FGF-2-induced activation of Erk1/2

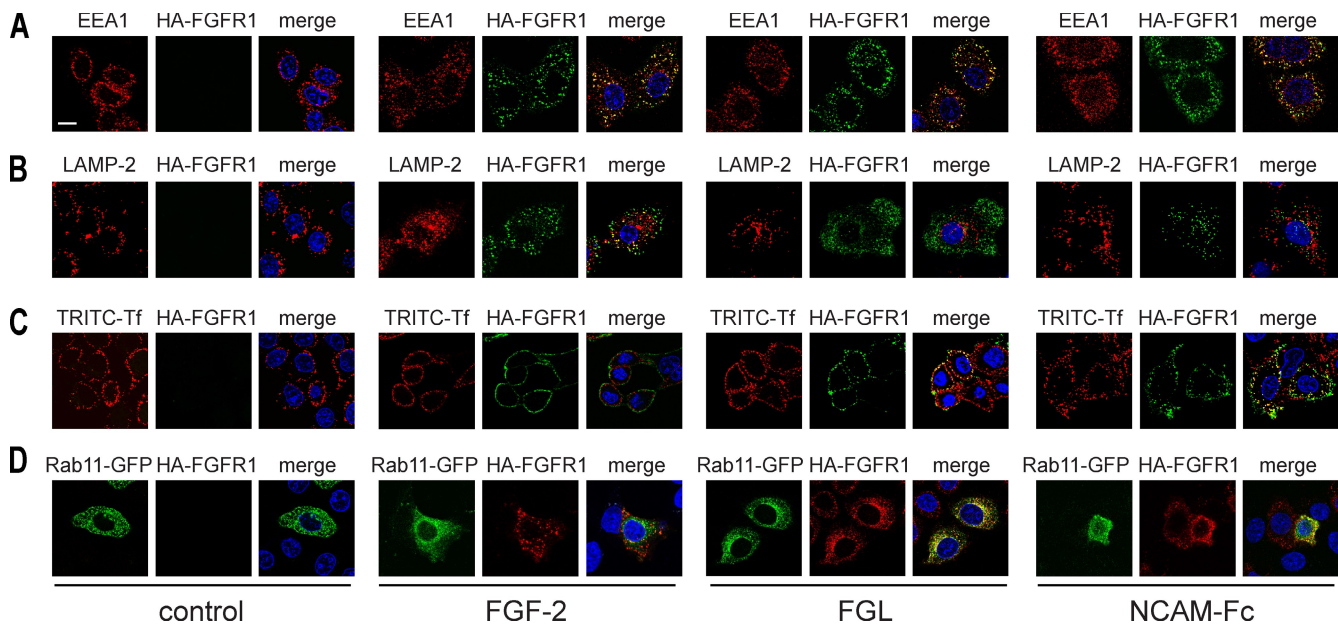


**Figure 5. Colocalization of HA-FGFR1 with different intracellular markers in FGF and NCAM-stimulated cells.** (A–C) HA-FGFR1–transfected HeLa cells were incubated with anti-HA antibody (green) and stimulated with FGF-2, FGL, or NCAM-Fc for 10 (A), 30 (C), or 60 min (B). In C, TRITC-Tf (red) was added together with the stimuli. After acid wash, cells were stained with anti-EEA1 (A) or anti-LAMP-2 (B) antibodies (red) as indicated. (D) HeLa cells cotransfected with HA-FGFR1 (red) and Rab11-GFP (green) were incubated with anti-HA antibody and stimulated with FGF-2, FGL, or NCAM-Fc for 60 min. After acid wash, cells were stained with Cy3-conjugated anti–mouse antibody. Yellow staining indicates the colocalization of HA-FGFR1 with endosomal markers. Bar, 10  $\mu$ m.

(Fig. 8, D and E). To further validate and extend these findings, FGFR1 recycling was inhibited by two additional approaches, namely cell pretreatment with monensin (Mitchell et al., 2004) and a temperature shift to 16°C (Ren et al., 1998). Both strategies showed efficient repression of NCAM-dependent recycling of HA-FGFR1 (Fig. S5, B and C), and in both cases, FGL was no longer able to stimulate cell migration, whereas recycling inhibition had no effect on EGF-induced migration (Fig. 8, F and G). Furthermore, blocking FGFR1 recycling at 16°C resulted in the loss of NCAM-stimulated activation of Src (Fig. S5 D). This was not caused by temperature-dependent inactivation of FGFR1, as under the same conditions, FGF-2 retained the ability to induce sustained Erk1/2 phosphorylation (Fig. S5 D). Thus, NCAM-induced, FGFR1-mediated signal transduction underlying cell migration relies on the recycling of the receptor. Collectively, these results support the notion that NCAM promotes cell migration by favoring a sustained and efficient recycling of internalized FGFR1 to the cell surface.

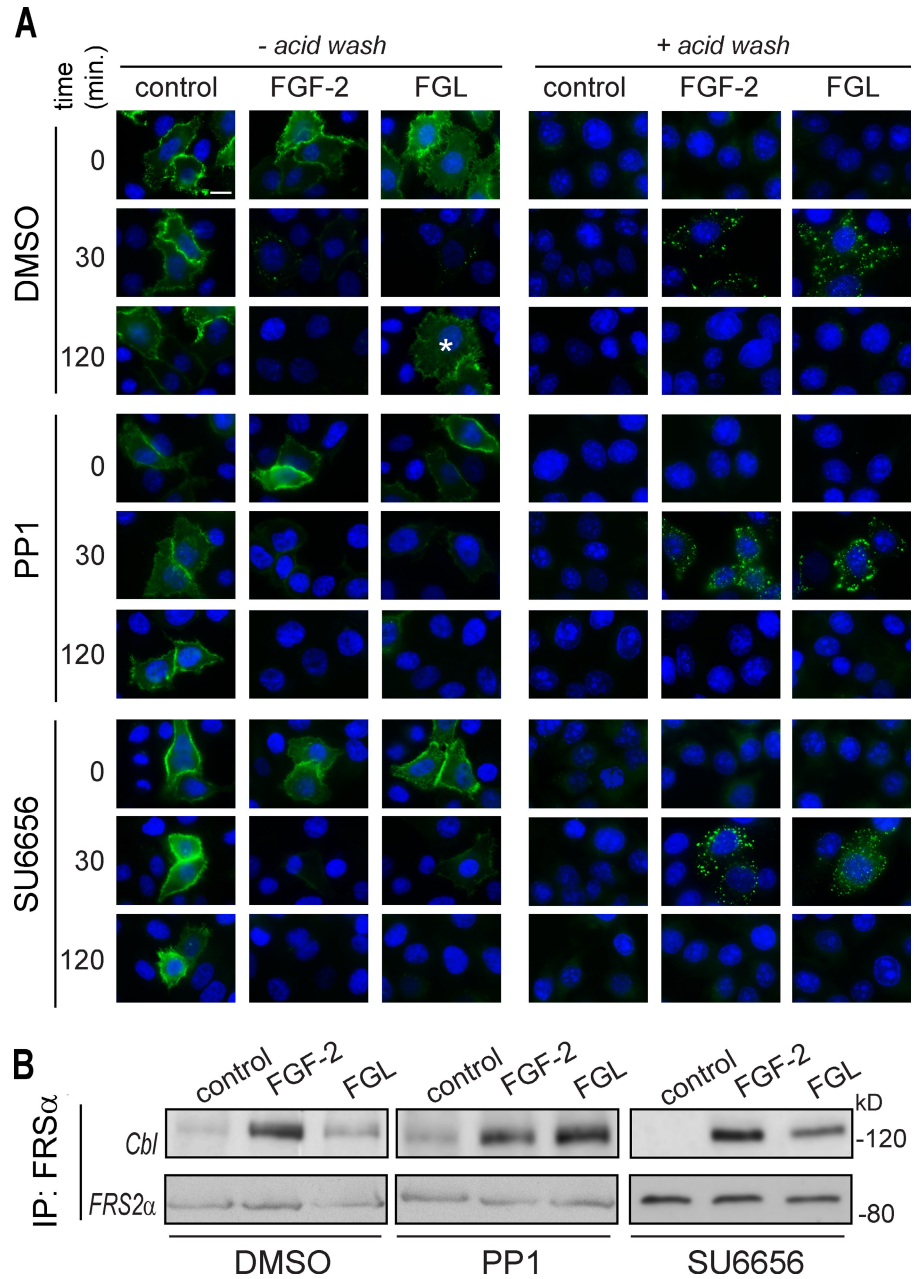
If the different cellular response to NCAM and FGF depends on the different stability and intracellular fate of FGFR1 imposed by the two ligands, one should be able to switch FGF into an NCAM-like stimulus by modulating FGFR1 stability. To verify this hypothesis, HeLa cells expressing a dn version of Cbl (Penengo et al., 2006) or wild-type Cbl as a control were stimulated with either FGF-2 or FGL. The inhibitory effect of dn-Cbl was confirmed by the fact that FGFR1 level was no longer reduced after a 120-min treatment with FGF-2 (Fig. 9 A). The dn-Cbl–dependent stabilization of FGFR1 resulted in the recycling of the receptor to the cell surface even after FGF-2 stimulation (Fig. 9 B), which is in contrast to the receptor degradation observed in parental HeLa cells (Fig. 3) or in cells

transfected with wild-type Cbl (Fig. 9 B). Notably, the expression of dn-Cbl enabled FGF-2 to induce HeLa cell migration, although not to the same extent as FGL (Fig. 9 C). Furthermore, under these conditions, FGF-2 stimulated sustained Src activation to a similar level as FGL (Fig. S5 E). Thus, the inhibition of Cbl-dependent ubiquitination and degradation of FGFR1 was sufficient to switch the functional properties of FGF-2, enabling it to mimic NCAM-induced cell migration and sustained signaling. This implies that the biological activity of FGFR1 is strictly dependent on its stability and trafficking. However, although interfering with FGFR1 degradation resulted in a migratory response to FGF-2, the blockade of FGFR1 recycling with dn-Rab11 (Fig. S5 F) did not confer proliferative function to NCAM (Fig. 9 D). This suggests that additional events are required to trigger the FGFR1-mediated signaling cascade that underlies the proliferative response.

## Discussion

The functional cross talk between NCAM and FGFR signaling in neurons has long been described (Williams et al., 1994). However, the molecular aspects of the interaction between the two molecules and, more importantly, the cellular response elicited by this interaction in nonneural cells, have remained elusive. This study shows that NCAM acts as a noncanonical ligand for FGFR and stimulates an FGFR-mediated cellular response that is remarkably distinct from that elicited by FGF. In particular, NCAM promotes sustained FGFR signaling and cell migration, which are two processes that require NCAM-dependent recycling of endocytic FGFR1 to the cell surface (whereas the receptor is degraded upon FGF stimulation). The dichotomy

**Figure 6. Src inhibition blocks the recycling of FGFR1 and promotes the association of Cbl with FRS-2 $\alpha$  in NCAM-stimulated cells.** (A) HeLa cells stimulated with FGF-2 or FGL in the presence of DMSO (top), PP1 (middle), or SU6656 (bottom) were processed as for Fig. 3 A. Asterisk marks a cell where HA-FGFR1 recycled back to the cell surface. Bar, 10  $\mu$ m. (B) HeLa cells were treated with DMSO (left), PP1 (middle), or SU6656 (right) before stimulation with either FGF-2 or FGL for 10 min. Cell extracts were immunoprecipitated (IP) with anti-FRS-2 $\alpha$  antibody and immunoblotted for Cbl (top) followed by immunoblotting for FRS-2 $\alpha$  (bottom).



with FGF-induced response did not depend on the ligand concentration used in the experiments (unpublished data).

To perform a direct comparison with the extracellular, soluble factor FGF-2, most of the experiments described in this study were conducted using either the FGL peptide or NCAM-Fc, namely soluble versions of NCAM-derived ligands. Despite NCAM acting mainly as a cell surface molecule, there is evidence indicating that FGL and NCAM-Fc recapitulate physiological activities of membrane-associated NCAM, thus supporting the biological relevance of our observations. First, soluble NCAM fragments mimicked cell surface NCAM in inducing FGFR-dependent matrix adhesion in different cell types (Cavallaro et al., 2001; this study). Second, in line with our findings on NCAM-Fc and FGL as promigratory factors, membrane NCAM induces cell migration in neurons (Maness and Schachner, 2007) and during epithelial-mesenchymal transition

(Lehembre et al., 2008). Finally, as discussed in Results, NCAM's ectodomain or fragments thereof are also released by certain cell types in vivo as soluble molecules, thus generating potential FGFR ligands analogous to NCAM-Fc and FGL. The oligomeric (FGL) or dimeric (NCAM-Fc) state of NCAM fragments are also likely to mimic physiological conditions, as NCAM is known to oligomerize by means of cis-homophilic interactions (Kiselyov et al., 2005).

The stimulation of FGFR with soluble NCAM underscores the importance of trans-interactions between the two molecules, as it would occur upon contact between NCAM- and FGFR-expressing cells or upon binding of shed extracellular domains of NCAM to cell surface FGFR. Nevertheless, the detection of NCAM-FGFR complexes on the surface of single cells (Cavallaro et al., 2001; Sanchez-Heras et al., 2006; Francavilla et al., 2007) indicates that the two proteins can also



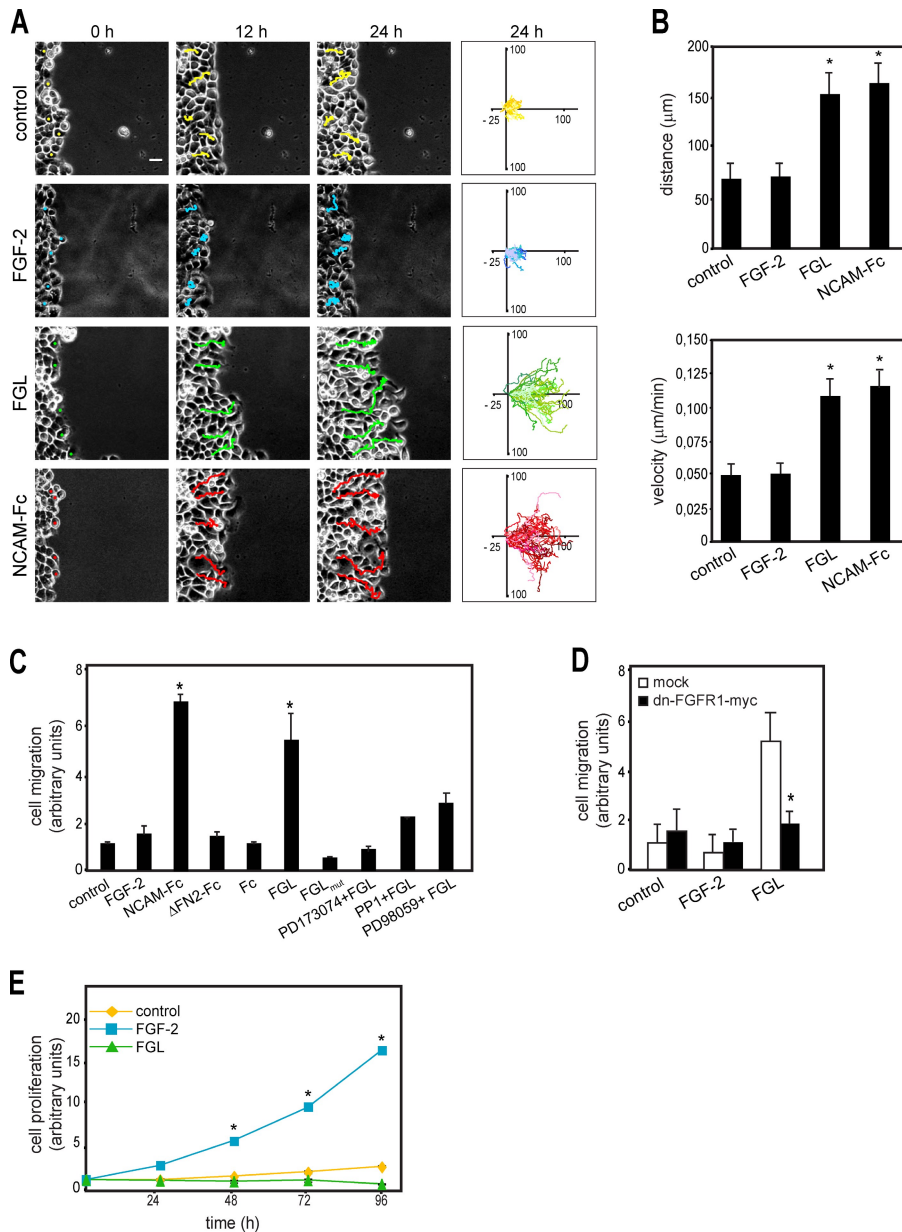


**Figure 7. NCAM induces cell migration via FGFR1, Src, and Erk1/2, whereas FGF promotes cell proliferation.** (A) Monolayers of HeLa cells were scratch wounded as described in Materials and methods and left untreated (control) or stimulated with FGF-2, FGL, or NCAM-Fc. Time-lapse microscopy was performed as described in Materials and methods. Images were taken from Videos 1–4. Colored lines show five representative tracks of single cells. Plots in the right column show the trajectories of 45 individually tracked cells over the 24-h period (see Materials and methods). Values are expressed in micrometers. Bar, 30 μm. (B) Mean distance covered (top) and velocity (bottom) of cells stimulated with the different ligands. Data represent the mean ± SEM from 45 individually tracked cells from three independent experiments. (C) HeLa cells stimulated with FGF-2, FGL, NCAM-Fc, ΔFN2-Fc, or Fc were subjected to migration assays in modified Boyden chambers (see Materials and methods). FGL stimulation was also performed in the presence of PD173074, PP1, or PD98059. (D) HeLa cells transfected with an empty vector (mock) or with Myc-tagged dn-FGFR1 (transfection efficiency was nearly 100%; not depicted) were stimulated with either FGF-2 or FGL and subjected to migration assay as for C. (E) HeLa cells were subjected to cell proliferation assay in the presence of FGF-2 or FGL as described in Materials and methods. (C–E) Data represent the mean ± SEM from at least three independent experiments. \*,  $P < 0.005$  relative to untreated cells.

engage in cis-interactions. Although we did not detect significant differences in signaling or cell matrix adhesion elicited by transmembrane NCAM versus soluble NCAM-Fc, cis- and trans-interactions between NCAM and FGFR could induce a different spectrum of FGFR-mediated cellular responses.

NCAM is unlikely to exert its FGFR-stimulating role by enhancing the function of endogenous FGFs given that, on one hand, it does not bind to FGF-2 and, on the other hand, NCAM actually inhibits the binding of FGF-2 to FGFR (Francavilla et al., 2007). These observations, combined with the evidence of a physical interaction between NCAM and FGFR (Kos and Chin, 2002; Kiselyov et al., 2003; Christensen et al., 2006; this study), point to NCAM-autonomous stimulation of FGFR activity. Thus, the mechanism whereby NCAM regulates FGFR signaling is remarkably different from that of other adhesion molecules, which instead affect the interaction of FGF with its receptor. For example, N- and E-cadherin regulate FGF-induced endocytosis of

FGFR1, impacting on ligand-dependent signaling (Suyama et al., 2002; Bryant et al., 2005). Unlike cadherins, the clustering of integrins does stimulate ligand-independent activation of RTKs (including EGFR, VEGFR, and PDGF receptor) as a result of the cis-interactions between integrins and RTKs themselves (Walker et al., 2005). Because NCAM-Fc is expected to act as a dimer (as a result of spontaneous Fc dimerization) and the FGL peptide was used in its dendrimeric form (Kiselyov et al., 2003), both molecules could induce FGFR1 activation by clustering, which is similar to cis-interacting integrins.

The molecular basis of the divergence between NCAM- and FGF-induced FGFR signaling remains elusive and could entail different mechanisms. For example, the two molecules could promote the autophosphorylation of different FGFR's tyrosine residues and, therefore, the activation of different docking sites for the specific effectors. Also, it remains to be clarified whether NCAM induces the recruitment of the receptor to

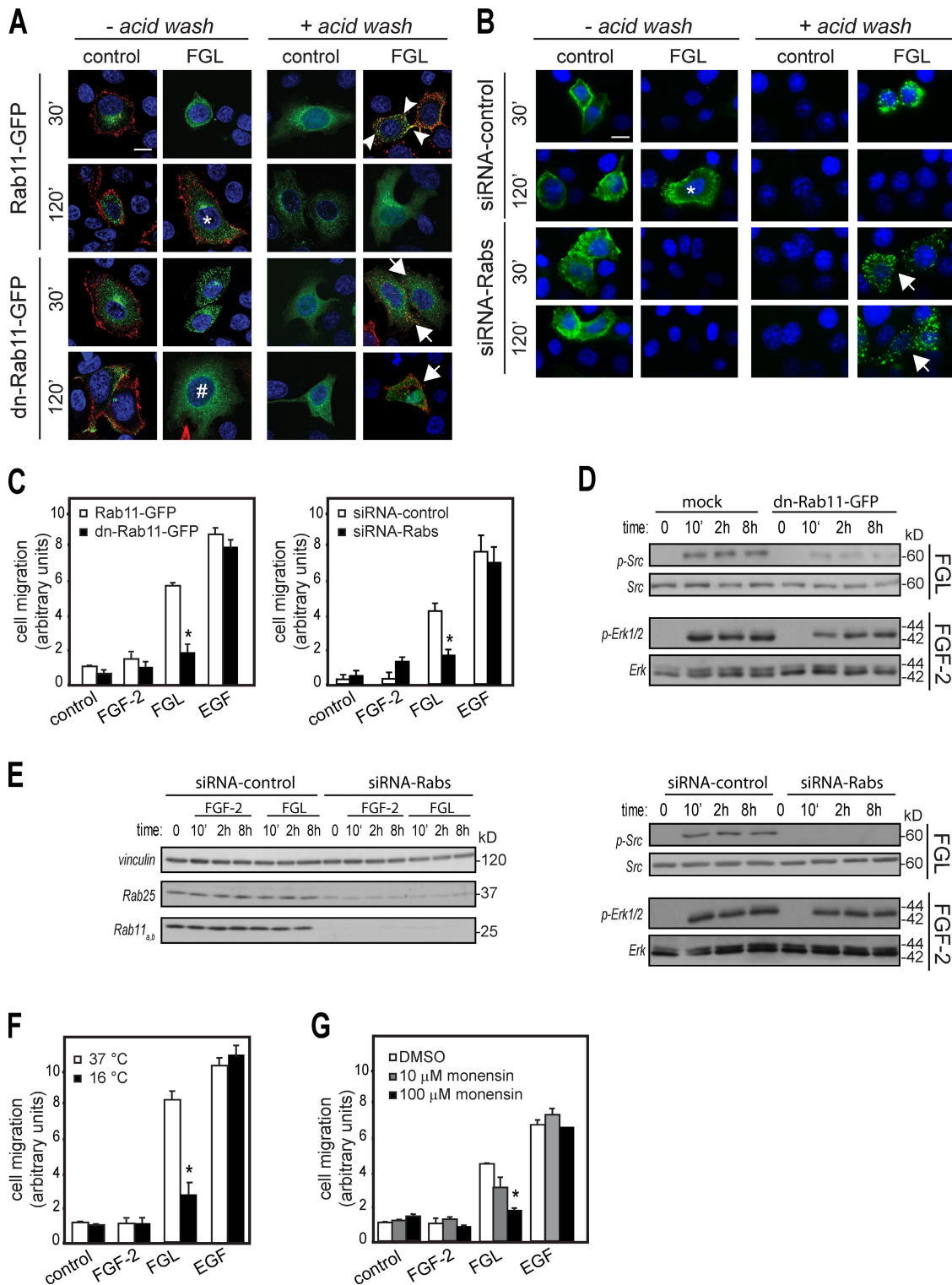


Figure 8. **Inhibition of FGFR1 recycling represses NCAM-induced cell migration.** (A) HeLa cells cotransfected with HA-FGFR1 (red) and either Rab11-GFP or dn-Rab11-GFP (green) were processed as for Fig. 3 A. Arrowheads indicate the colocalization of Rab11-GFP with HA-FGFR1 (yellow staining), whereas arrows indicate the lack of colocalization of HA-FGFR1 with dn-Rab11-GFP. Asterisk indicates a Rab11-GFP-expressing cell with recycled HA-FGFR1, whereas # shows a dn-Rab11-GFP-expressing cell with no recycling of HA-FGFR1. (B) HeLa cells were transfected with control siRNA (top) or with a mixture of siRNA targeting the Rab11 family (bottom) before transfection with HA-FGFR1 (green) and processing as for Fig. 3 A. Arrows indicate cells transfected with anti-Rab11 siRNA with no recycling of HA-FGFR1 upon FGL stimulation, whereas the asterisk shows a control cell where HA-FGFR1 has recycled to the cell surface. Bars, 10 μm. (C, left) HeLa cells transfected with either Rab11-GFP or dn-Rab11-GFP were stimulated with FGF-2, FGL, or EGF, and the migration of GFP-positive cells in modified Boyden chambers was measured. (right) HeLa cells were transfected with either control or anti-Rab11 siRNA and stimulated and subjected to migration assay as described for the left panel. \*,  $P < 0.005$  relative to cells transfected with either Rab11-GFP (left) or control siRNA (right) and stimulated with FGL. (D) HeLa cells transfected with either Rab11-GFP or dn-Rab11-GFP were stimulated with FGL (top) or FGF-2 (bottom) for the indicated time lengths. Lysates from FGL-stimulated cells were immunoblotted for phospho-Src and total Src, whereas lysates from

specific membrane compartments where the repertoire of adaptors/effectors would be different from that normally affected by FGF stimulation.

The dichotomy in FGFR signaling between NCAM and FGF is best exemplified by the pathway of Erk1/2 activation (Ras-dependent for FGF and Ras-independent and Src-dependent for NCAM) and by the differential involvement of Shc and Src downstream of FGFR (specifically activated by FGF and NCAM, respectively). Src-mediated activation of Erk1/2 can result from integrin signaling through focal adhesion kinase (Mittra and Schlaepfer, 2006). Because NCAM–FGFR signaling stimulates  $\beta_1$ -integrin function in pancreatic  $\beta$ -tumor cells (Cavallaro et al., 2001), NCAM-induced activation of FGFR could trigger an integrin–FAK–Src–Erk1/2 pathway. This model would be supported by the observation that, similar to NCAM, integrin-mediated activation of Erk1/2 is independent of Ras (Chen et al., 1996), although this issue is still controversial (Clark and Hynes, 1996).

The divergence between NCAM and FGF signaling is accompanied by a dramatic difference in the intracellular trafficking of FGFR1, with FGF inducing the classical route of rapid internalization and lysosomal degradation, whereas NCAM promotes FGFR1 stabilization and recycling to the cell surface. We have provided evidence that NCAM stimulation uncouples receptor internalization from ubiquitination, most likely because NCAM does not induce the recruitment of Cbl to FRS-2 $\alpha$ , which is required for FGFR1 ubiquitination and degradation upon FGF stimulation (Wong et al., 2002). Recent studies showed that preventing ubiquitination targets FGFR1 to recycling endosomes instead of lysosomes (Haugsten et al., 2008), further supporting the view that this is the mechanism underlying NCAM-dependent recycling of FGFR1. The sharp dichotomy in the intracellular fate of FGFR1 after FGF versus NCAM stimulation is likely determined by Src activity. Indeed, Src prevents the association of Cbl with FRS-2 $\alpha$  and, thus, the ubiquitination of FGFR1, thus accounting for the lack of receptor degradation and for its recycling to the cell surface. However, our unpublished results ruled out the possibility that Src induces the phosphorylation of Cbl in NCAM-stimulated cells, thus hindering its recruitment to FRS-2 $\alpha$  (unpublished data). It is conceivable that NCAM stimulation promotes Src-dependent phosphorylation of one or more substrates that in turn interfere with the formation of the Cbl–FRS-2 $\alpha$  complex, which is a hypothesis that deserves further investigation. In parallel with Src-dependent FGFR recycling, we also observed that the sustained activation of Src induced by NCAM requires FGFR recycling itself. This points to a mutual regulation between the two events as a key step in the cellular response elicited by the NCAM–FGFR interplay.

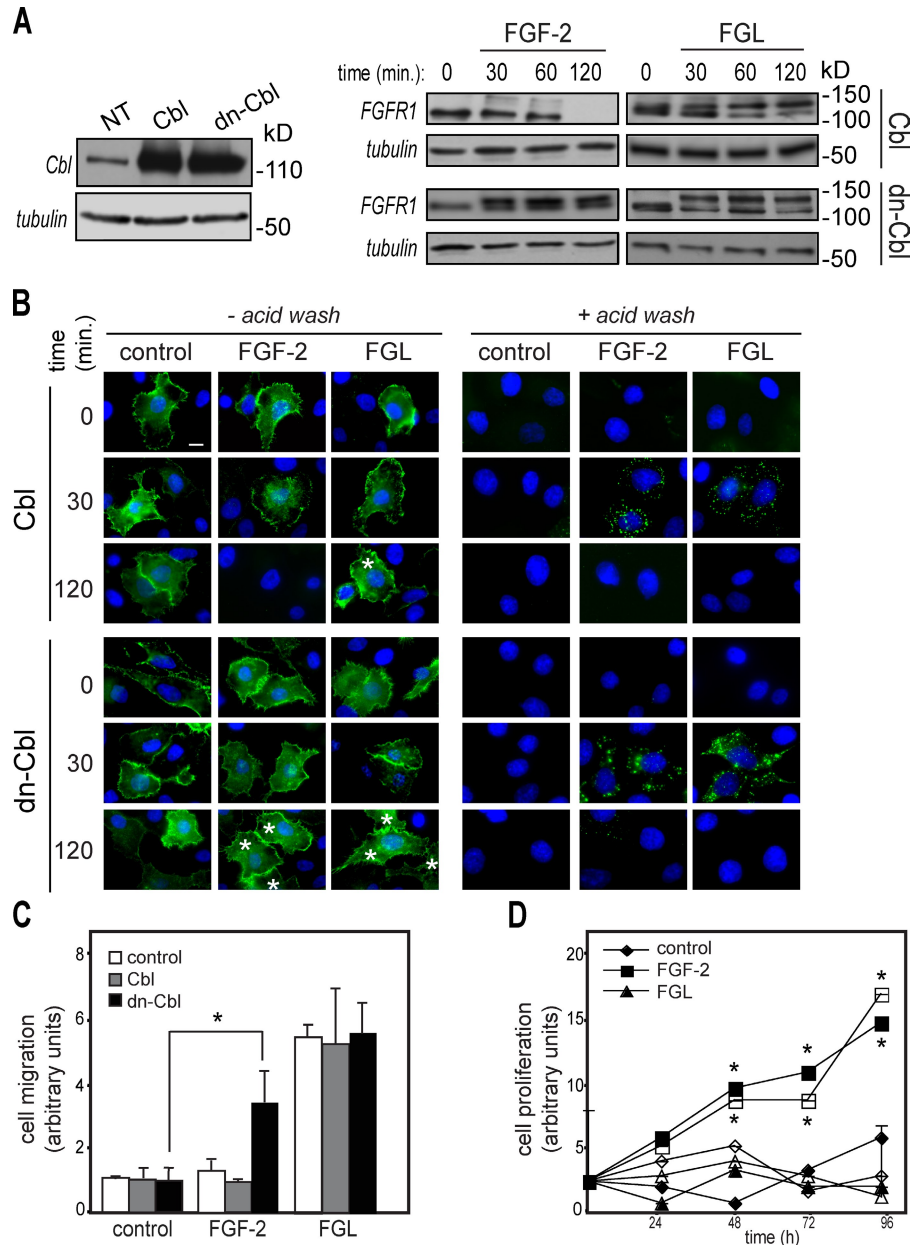
Our study revealed the tight connection between recycling of FGFR1 to the plasma membrane and NCAM-induced cell migration. Interestingly, transmembrane NCAM itself undergoes endocytosis and recycling in neurons (Diestel et al., 2007). Although the biological significance of these processes remains elusive, it is tempting to speculate that NCAM could act as a carrier for other proteins and in particular for FGFR, thus favoring their recycling to the cell surface. Despite the copious evidence that endocytosis is used by cells to propagate RTK-mediated signaling from endosomal compartments (Hoeller et al., 2005), very few studies have focused on RTK recycling (Marmor and Yarden, 2004), and little information is available on its biological significance. Recycling of EGFR and PDGF/VEGFR is critical for the spatial redistribution of RTK signaling during the directional migration of border cells in *Drosophila melanogaster* (Jékely et al., 2005). The role of recycling in ensuring localized signaling during cell migration has also been reported for the small GTPase Rac (Palamidessi et al., 2008) and for integrins (for review see Caswell and Norman, 2008). Future research should clarify whether FGFR1 recycling in NCAM-stimulated migratory cells is necessary to restrict receptor localization to specific membrane compartments or if it rather represents a mechanism to avoid degradation and ensure the sustained signaling required to maintain a motile phenotype. In this context, it appears that the duration of NCAM-dependent FGFR signaling is critical to confer a migratory phenotype to cells. This was further confirmed by our observation that preventing FGFR1 ubiquitination and degradation, thus promoting its recycling, was sufficient to confer promigratory activity to FGF-2. Thus, the cellular response to FGF-2 is dictated by the stability of FGFR1, which in turn affects the duration of downstream signaling. In agreement with this view, forcing the sustained activation of FGFR2 induces epithelial to mesenchymal transition and cellular invasion (Xian et al., 2007).

Our results on the NCAM–FGFR1 interplay that induces recycling-dependent cell migration have broad physiopathological implications. For example, NCAM-dependent sustained activation and recycling of FGFR are very likely to underlie axonal growth, a process that requires an intact FGFR signaling downstream of NCAM both in vitro and in vivo (Saffell et al., 1997). NCAM knockout mice exhibit various developmental and behavioral defects, including the impaired migration of neuronal precursors to the olfactory bulb (Cremer et al., 1994). Our findings imply that these defects might depend on the disruption of promigratory FGFR signaling upon loss of NCAM. In this context, NCAM-deficient mice exhibit a depression-like phenotype that is reverted by the treatment with FGL (Aonurm-Helm et al., 2008). These findings support the physiological relevance of the NCAM–FGFR interaction for brain development

---

FGF-2-stimulated cells were immunoblotted for phospho-Erk1/2 and total Erk1/2. (E) HeLa cells transfected with either control or anti-Rab11 siRNA were stimulated with FGF-2 or FGL for the indicated time lengths. Knockdown was verified by immunoblotting for Rab11a/Rab11b and for Rab25 using vinculin as a loading control (left). Lysates from stimulated cells were immunoblotted for activated Src or Erk1/2 as described for D. (F) HeLa cells were cultured at 37 or 16°C, stimulated with FGF-2, FGL, or EGF, and subjected to migration assay in modified Boyden chambers. \*,  $P < 0.005$  relative to cells grown at 37°C and stimulated with FGL. (G) HeLa cells stimulated with FGF-2, FGL, or EGF in the presence of either DMSO or monensin (10 or 100  $\mu$ M) were subjected to migration assay in modified Boyden chambers. \*,  $P < 0.005$  relative to DMSO-treated cells stimulated with FGL. Data represent the mean  $\pm$  SEM from three independent experiments.

**Figure 9. Inhibition of Cbl-mediated FGFR1 degradation results in FGF-2-induced cell migration.** (A, left) Lysates from HeLa cells stably transfected with Cbl or dn-Cbl were immunoblotted for Cbl using tubulin as loading control. (right) Transfected cells were stimulated with FGF-2 or FGL in the presence of cycloheximide for the indicated time intervals followed by lysis and immunoblotting for FGFR1 using tubulin as loading control. NT, not transfected. (B) HeLa cells stably expressing either wild-type Cbl or dn-Cbl were transfected with HA-FGFR1. Cells were incubated with anti-HA antibody and stimulated with either FGF-2 or FGL. Cells were processed as for Fig. 3 A. Asterisks mark cells where HA-FGFR1 recycled back to the cell surface. Bar, 10  $\mu$ m. (C) HeLa cells stably transfected with either wild-type Cbl (gray bars) or dn-Cbl (black bars) and nontransfected cells (white bars) were stimulated with FGF-2 or FGL before migration assay in modified Boyden chambers. (D) HeLa cells transfected with an empty vector (open symbols) or with GFP-tagged dn-Rab11 (closed symbols) were serum starved and stimulated with FGF-2 or FGL for the indicated time intervals. Cell proliferation was determined as described in Materials and methods. \*,  $P < 0.005$  relative to untreated cells. Data represent the mean  $\pm$  SEM from three independent experiments.



and plasticity. Notably, although NCAM knockout mice are viable and reach adulthood, the transgenic expression of the soluble NCAM's ectodomain in the same mice results in dominant embryonic lethality (Rabinowitz et al., 1996). This implies that NCAM heterophilic interactions require a tight regulation during embryonic development, and we speculate that excessive stimulation of FGFR by soluble NCAM contributes to the phenotype of mutant mice. Finally, the aberrant expression of NCAM is a hallmark of various neoplastic diseases (Zecchini and Cavallaro, 2008), and the sustained activation of FGFR (as found in various cancer types; Acevedo et al., 2009) might underlie a proinvasive role of NCAM during tumor progression. This hypothesis is supported by our recent data implicating the NCAM-FGFR interplay as a causal factor in ovarian carcinoma (unpublished data).

In summary, we have unraveled a novel mechanism of FGFR activation involving the interaction with NCAM that,

acting as an unconventional ligand, stimulates a signaling cascade remarkably distinct from that induced by FGF. Furthermore, our experiments revealed that NCAM induces sustained FGFR activation by uncoupling receptor internalization from ubiquitination and promoting Rab11-dependent recycling of the receptor, and this results in cell migration. Besides uncovering a further level of complexity in the regulation of RTK activity, our data could contribute to elucidate the pathogenesis of those disorders characterized by dysregulated function of NCAM and/or FGFR.

## Materials and methods

### Reagents

The following commercial reagents were used: FGF-2 (PeproTech), EGF (Inalco), the MEK inhibitor PD98059, the inhibitor of transport to plasma membrane monensin, the protein synthesis inhibitor cycloheximide

(Sigma-Aldrich), and the Src inhibitors PP1 and SU6656 (EMD). The FGFR inhibitor PD173074 [Skaper et al., 2000] was provided by Pfizer. The EGFR inhibitor AG1478 was obtained from Sigma-Aldrich.

The following antibodies were used: rabbit anti-phospho-Akt and anti-Akt; mouse anti-phospho-Erk1/2, rabbit anti-phospho-FRS-2 $\alpha$ , rabbit anti-phospho-Src (recognizing the activated form of most Src kinases), rabbit anti-phospho-PLC- $\gamma$ , anti-phospho-Shc, and anti-Shc (Cell Signaling Technology); rabbit anti-Erk1/2 and mouse antitubulin and antivinculin (Sigma-Aldrich); mouse anti-HA (clone F7; used in immunoprecipitation and Western blot analysis); rabbit anti-FGFR1, anti-FGFR2, anti-FGFR3, anti-FGFR4, rabbit anti-FRS-2 $\alpha$ , mouse anti-NCAM (clone 123C3), anti-Src kinases, anti-GFP, antiubiquitin, and anti-Rab25; goat anti-EEA1 (Santa Cruz Biotechnology, Inc.); mouse anti-PLC- $\gamma$ , anti-Cbl, and anti-phosphotyrosine (BD); mouse anti-HA tag (used in immunofluorescence; HA.11; Covance); and rabbit anti-Rab11, cross-reacting with both Rab11a and Rab11b (Invitrogen). Rabbit anti-LAMP-2 was provided by G. Griffiths (Cambridge Institute for Medical Research, Cambridge, England, UK).

The Myc-tagged scFv against FGFR1 was isolated and used in immunoblotting as described previously [Francavilla et al., 2007]. Peroxidase-conjugated streptavidin was obtained from Jackson ImmunoResearch Laboratories, and TRITC-conjugated Tf (TRITC-Tf) was obtained from Invitrogen. The FGL peptide from the second FNIII module of NCAM and its mutated version, FGL<sub>mut</sub>, which carries two alanine substitutions that abolish its binding to FGFR [Kiselyov et al., 2003], were provided by ENKAM Pharmaceuticals. Peptides were synthesized as dendrimers, with four peptides attached to a three-lysine backbone [Kiselyov et al., 2003].

### Expression vectors

The pIg3 vectors containing the cDNA for the ectodomain of human NCAM, either full-length or deleted of the second FNIII repeat ( $\Delta$ FN2), fused to the Fc fragment of human IgG (NCAM-Fc and  $\Delta$ FN2-Fc, respectively), were provided by L. Needham (Duke University, Durham, NC). The cDNA for full-length, transmembrane NCAM-140 was subcloned into a pRc/CMV vector. The pSecTag vector encoding the HA-Myc-His-tagged ectodomain of human NCAM was provided by D. Sjostrand (Stockholm, Sweden). The pRK5tkNEO vector encoding the ectodomain of human FGFR1 fused to human Fc was provided by A. Gurney (Genentech). These vectors were used to transiently transfect HEK293 cells, and the recombinant proteins were purified from the conditioned medium of transfected cells by affinity chromatography. The pDisplay vector encoding N-terminally HA-tagged FGFR1 [Zhang et al., 2001] was provided by G. David (Leuven, Belgium). The cDNA for dn-Ras (N17V), generated by J.S. Gutkind, was provided by G. Scita (IFOM, Milan, Italy). The cDNA for Rab11-GFP and dn-Rab11 (S25N)-GFP were obtained from F. Senic-Matuglia (IFOM, Milan, Italy) and B. Goud (Institut Curie, Paris, France). The cDNA encoding dn-FGFR1 [Werner et al., 1993] was subcloned into the pMex-neo vector. dn-Src (K295R and Y527F), generated by J. Brugge, was provided by M. Sallèse (Mario Negri Sud, Santa Maria Imbaro, Italy).

### Cell lines and transfection

Mouse fibroblastic L cells and human epithelial HeLa cells were cultured in DME supplemented with 10% fetal bovine serum, 2 mM L-glutamine, 100 U/ml penicillin, and 100  $\mu$ g/ml streptomycin at 37°C in a humidified incubator with 5% CO<sub>2</sub> [Francavilla et al., 2007; Palamidessi et al., 2008]. HeLa cells were transfected using Lipofectamine (Invitrogen) according to the manufacturer's instructions, and all of the assays were performed 36 h after transfection. HeLa cells stably transfected with wild-type or dn-Cbl [Penengo et al., 2006] were provided by S. Polo (Milan, Italy).

### RNAi

Double-stranded, validated Stealth siRNA oligonucleotides targeting Rab11a (5'-GGAGCUGUAGGUGCCUUAUUGGUUU-3') and Rab11b (5'-GACGACGAGUACGACUACCUAUUCA-3'; Arnaud et al., 2007) were purchased from Invitrogen. A pool of two siRNA duplexes against Rab25 (also known as Rab11c; 5'-CAUGCUCGUGGGUAAACAAA-3' and 5'-CUUCAUGCCCUAUCACAAA-3') was purchased from Santa Cruz Biotechnology, Inc. Cells were transfected with a mixture of all Rab11-targeting siRNAs as previously described [Francavilla et al., 2007]. An siRNA duplex against mouse NCAM [Francavilla et al., 2007] was used as a negative control. Silencing of gene expression was monitored by immunofluorescence and immunoblotting of cell lysates with antibodies against Rab11 (cross reacting with both a and b) or Rab25.

### Cell stimulation and immunoblotting

Cells were cultured in 6-well plates in complete medium and serum starved overnight in serum-free medium. Cells were stimulated for the indicated

time points with 40  $\mu$ g/ml FGL, 20  $\mu$ g/ml NCAM-Fc or  $\Delta$ FN2-Fc, or 20 ng/ml FGF-2. A mutated version of FGL unable to interact with FGFR [Kiselyov et al., 2003] was used in most assays as a control for FGL, and consistently showed no effect. When needed, cells were preincubated for 2 h with chemical inhibitors at the following concentrations: 100 nM PD173074, 25  $\mu$ M PD98059, 20  $\mu$ M PP1, 270 nM SU6656, 0.5  $\mu$ M AG1478, 25  $\mu$ M cycloheximide, and 10 or 100  $\mu$ M monensin. Control cells were preincubated with DMSO alone. After stimulation, cell extraction and immunoblotting were performed as described previously [Francavilla et al., 2007]. Each experiment was repeated at least three times.

### Cell surface biotinylation and immunoprecipitation

Internalization and recycling of FGFR1 were quantitatively evaluated as described previously [Fabbri et al., 1999; Lampugnani et al., 2006]. In brief, cells were plated at 80% confluence on 100-mm-diameter dishes and incubated on ice for 60 min in the presence of 0.5 mg/ml thiol-cleavable sulfo-NHS-S-S-biotin (Thermo Fisher Scientific). After washing, labeled cells were incubated at 37°C for the indicated time periods in the presence of FGF-2 or FGL to allow internalization. Cells were incubated on ice twice for 20 min with 45 mM GSH (glutathione; EMD), a membrane-nonpermeable reducing agent, to remove the biotin label from surface proteins. Free sulfo-reactive groups were quenched with iodoacetamide (Sigma-Aldrich). Total labeling was determined in samples not treated with GSH, whereas background values were obtained from samples not subjected to incubation at 37°C.

Immunoprecipitation of FGFR1 from cell extracts was performed as described previously [Cavallaro et al., 2001] using anti-FGFR1 (C15). After SDS-PAGE, immunoprecipitates were probed with HRP-conjugated streptavidin (to visualize biotinylated FGFR1) followed by stripping and immunoblotting for total FGFR1. Densitometric analysis was performed with the ImageJ software (National Institutes of Health). Internalization was calculated as a percentage of the total amount of labeled receptor.

FGFR1 recycling and degradation (Fig. 3 C) was determined as described previously [Fabbri et al., 1999]. In brief, cells were labeled with sulpho-NHS-S-S-biotin (as described in the previous paragraph), and internalization was allowed for 30 min at 37°C in the presence of the stimuli. Cells were treated with GSH (as described in the previous paragraph) to remove the label from the residual cell surface receptor. The internalized fraction was chased by reincubation at 37°C for the indicated time points in duplicate samples. One sample (Fig. 3 C, +GSH) was treated with GSH to determine the amount of FGFR1 that recycled back to the plasma membrane, whereas the other sample (-GSH) was left untreated to determine the total level of labeled receptor at each time point. The samples were subjected to FGFR1 immunoprecipitation and immunoblotting as described in the previous paragraph. In -GSH samples, HRP-conjugated streptavidin recognized residual biotinylated FGFR1 after incubation at 37°C without GSH treatment (i.e., internalized + recycled - degraded). In +GSH samples, HRP-conjugated streptavidin recognized residual biotinylated FGFR1 after incubation at 37°C and GSH treatment (i.e., internalized - recycled - degraded). FGFR1 degradation was calculated by subtracting the densitometric value of residual biotinylated receptor in -GSH samples from the total pool of internalized receptor. FGFR1 recycling was calculated by subtracting both the degradation value and the value of residual biotinylated receptor in +GSH samples from the total pool of internalized receptor [Lampugnani et al., 2006]. Values represent the means  $\pm$  SD from at least three independent experiments.

### Cell proliferation assays

Cells were seeded in triplicate on 24-well plates at 8  $\times$  10<sup>3</sup> cells/well, serum starved overnight, and treated for 1–4 d with FGF-2 or FGL replenished every 24 h. At each time point, viable cells were counted using the Trypan blue exclusion method, and the ratio with nonstimulated cells at time 0 was determined for each time point. Values represent the means  $\pm$  SEM from at least three independent experiments performed in triplicate.

### Cell migration

Time-lapse video microscopy was performed as described previously [White et al., 2007; Palamidessi et al., 2008] with slight modifications. In brief, confluent monolayers of serum-starved HeLa cells were wounded with a plastic pipette tip to induce migration into the wound. Cells were incubated in serum-free, Hepes-buffered L15 medium containing the different stimuli and placed on the stage of an inverted motorized microscope (IX81; Olympus) in a cage incubator (Okolab) at 37°C. Phase-contrast images were collected with a 10 $\times$  NA 0.3 UPlan lens (FLN; Olympus) every 15 min over a 24-h period using a camera (Orca-AG; Hamamatsu Photonics) and the cell<sup>AR</sup> software (Olympus). Videos were generated using the

ImageJ software for image analysis. Cell trajectories were determined using the manual tracking plugin of ImageJ. This procedure generated x and y coordinates for the center of each cell at each time point. Trajectories were reconstructed according to the recorded data. The distance covered by each cell and the migration speed were extracted from the track plots. 45 cells from three independent experiments were analyzed for each condition, and data are expressed in micrometers as mean  $\pm$  SEM.

#### Boyden chamber

Cell migration was measured using a two-chamber Transwell system (5- $\mu$ m pores; Costar). The top side of the filter was coated with polylysine. 40,000 serum-starved cells were seeded in the top well of Transwell in the presence of stimuli and, when indicated, of inhibitors. 400  $\mu$ l of complete medium was placed in the bottom chamber as chemoattractant. Migration was allowed for 16 h (L cells) or 24 h (HeLa cells) at 37 or 16°C. Cells remaining on the top surface of filters were scraped off. Cells on the bottom side were fixed with paraformaldehyde and stained with DAPI. Cells were counted in 10 random fields per filter using a microscope (Biosystem BX61; Olympus) with a 20 $\times$  NA 0.7 Plan Apo lens equipped with a camera (F-View II; Olympus) and the analysis software (Soft Imaging System GmbH). Results represent mean  $\pm$  SEM of at least three independent experiments for each cell types performed in triplicate.

#### Immunofluorescence

Immunofluorescence staining of live cells and postfixation were performed as described previously (Di Guglielmo et al., 2003; Martínez-Arca et al., 2005). In brief, HA-FGFR1-transfected HeLa cells were incubated on ice with 10  $\mu$ g/ml anti-HA antibody for 45 min with gentle agitation. We verified that the binding of the antibody did not activate HA-FGFR1 signaling in untreated cells. Moreover, the antibody did not induce HA-FGFR1 internalization (Fig. 3 A, control). After adding FGF-2, NCAM-Fc, or FGL, cells were incubated at 37°C for different time periods. At each time point, non-permeabilized cells were either fixed to visualize the receptor on the cell surface or acid washed in ice-cold buffer (50 mM glycine, pH 2.5) to remove surface-bound antibody. Cells were fixed and permeabilized to visualize the internalized receptor. Samples treated with TRITC-Tf (added to the medium at a final concentration of 50  $\mu$ g/ml) were kept in the dark. Finally, to detect HA-FGFR1, cells were stained with Alexa Fluor 488-conjugated donkey anti-mouse (Jackson ImmunoResearch Laboratories). Coverslips were mounted in 10% Mowiol (Kuraray Europe GmbH), and images were collected at room temperature using a microscope (Biosystem BX61) with a 100 $\times$  1.4 NA Plan Apo oil lens. For each time point and each treatment, the presence and localization (i.e., cell surface vs. internalized) of HA-FGFR1 were assessed in seven randomly chosen fields. Approximately 100 cells per treatment were analyzed for each time point from three independent experiments. The ratio between the number of HA-FGFR1-positive cells and total cells (corresponding to DAPI-stained nuclei) was determined and referred to the values obtained at time 0. For colocalization experiments, cells were permeabilized with 0.02% saponin (Sigma-Aldrich), treated with primary antibodies for 1 h at 37°C, and stained with Alexa Fluor 488-conjugated donkey anti-mouse together with CY3-conjugated donkey anti-rabbit or donkey anti-goat secondary antibodies.

When cells were transfected with GFP-containing plasmids, a CY3-conjugated goat anti-mouse secondary antibody was used. Images were acquired at room temperature from single confocal planes using an acousto-optical beam splitter confocal microscope (TCS SP2; Leica) and illumination from a 405-nm laser diode, a 488-nm argon laser, a 561-nm solid-state laser, and a 633-nm HeNe laser. We used a 63 $\times$  1.40 NA Plan Apo oil lens (HCX; Leica) and a 3.7 $\times$  zoom. Images were acquired using confocal software (Leica) and processed with Photoshop (version CS3; Adobe).

#### Online supplemental material

Fig. S1 shows that NCAM binds directly to FGFR1 and promotes FGFR-mediated cell adhesion. Fig. S2 shows that NCAM and FGF stimulate distinct signaling pathways downstream of FGFR. Fig. S3 shows the characterization and quantification of FGFR1 internalization, degradation, and recycling upon stimulation with FGL or FGF-2. Fig. S4 shows that Src inhibition results in FGL-induced ubiquitination of FGFR1 and that NCAM induces L cell migration via FGFR1, Src, and Erk1/2. Fig. S5 shows that FGF1 recycling is required for NCAM-induced cell migration. Videos 1–4 show the migration of HeLa cells either unstimulated or stimulated with FGF-2, FGL, or NCAM-Fc. Online supplemental material is available at <http://www.jcb.org/cgi/content/full/jcb.200903030/DC1>.

We are grateful to ENKAM Pharmaceuticals A/S, Pfizer, G. Scita, J. Brugge, M. Sallèse, G. David, L. Needham, G. Griffiths, D. Sjöstrand, F. Senic-Matug-

lia, and B. Goud for providing reagents and to D. Piccini for performing the solid phase-binding assays. We thank P.P. Di Fiore, S. Polo, and G. Scita for critical comments and suggestions.

This work was supported by research grants from Associazione Italiana Ricerca sul Cancro, the Association for International Cancer Research, Fondazione Cariplo, Fondazione Telethon, and the Italian Ministry of Health.

Submitted: 6 March 2009

Accepted: 23 November 2009

## References

- Acevedo, V.D., M. Ittmann, and D.M. Spencer. 2009. Paths of FGFR-driven tumorigenesis. *Cell Cycle*. 8:580–588.
- Aonurm-Helm, A., M. Jurgenson, T. Zharkovsky, K. Sonn, V. Berezin, E. Bock, and A. Zharkovsky. 2008. Depression-like behaviour in neural cell adhesion molecule (NCAM)-deficient mice and its reversal by an NCAM-derived peptide, FGL. *Eur. J. Neurosci.* 28:1618–1628. doi:10.1111/j.1460-9568.2008.06471.x
- Arnaud, F., P.R. Murcia, and M. Palmarini. 2007. Mechanisms of late restriction induced by an endogenous retrovirus. *J. Virol.* 81:11441–11451. doi:10.1128/JVI.01214-07
- Beenken, A., and M. Mohammadi. 2009. The FGF family: biology, pathophysiology and therapy. *Nat. Rev. Drug Discov.* 8:235–253. doi:10.1038/nrd2792
- Boilly, B., A.S. Vercoutter-Edouart, H. Hondermarck, V. Nurcombe, and X. Le Bourhis. 2000. FGF signals for cell proliferation and migration through different pathways. *Cytokine Growth Factor Rev.* 11:295–302. doi:10.1016/S1359-6101(00)00014-9
- Bryant, D.M., F.G. Wylie, and J.L. Stow. 2005. Regulation of endocytosis, nuclear translocation, and signaling of fibroblast growth factor receptor 1 by E-cadherin. *Mol. Biol. Cell.* 16:14–23. doi:10.1091/mbc.E04-09-0845
- Caswell, P., and J. Norman. 2008. Endocytic transport of integrins during cell migration and invasion. *Trends Cell Biol.* 18:257–263. doi:10.1016/j.tcb.2008.03.004
- Cavallaro, U., and G. Christofori. 2004. Cell adhesion and signalling by cadherins and Ig-CAMs in cancer. *Nat. Rev. Cancer.* 4:118–132.
- Cavallaro, U., J. Niedermeyer, M. Fuxa, and G. Christofori. 2001. N-CAM modulates tumour-cell adhesion to matrix by inducing FGF-receptor signalling. *Nat. Cell Biol.* 3:650–657. doi:10.1038/35083041
- Chen, J.W., T.L. Murphy, M.C. Willingham, I. Pastan, and J.T. August. 1985. Identification of two lysosomal membrane glycoproteins. *J. Cell Biol.* 101:85–95. doi:10.1083/jcb.101.1.85
- Chen, Q., T.H. Lin, C.J. Der, and R.L. Juliano. 1996. Integrin-mediated activation of MEK and mitogen-activated protein kinase is independent of Ras [corrected]. *J. Biol. Chem.* 271:18122–18127. doi:10.1074/jbc.271.30.18122
- Christensen, C., J.B. Lauridsen, V. Berezin, E. Bock, and V.V. Kiselyov. 2006. The neural cell adhesion molecule binds to fibroblast growth factor receptor 2. *FEBS Lett.* 580:3386–3390. doi:10.1016/j.febslet.2006.05.008
- Clark, E.A., and R.O. Hynes. 1996. Ras activation is necessary for integrin-mediated activation of extracellular signal-regulated kinase 2 and cytosolic phospholipase A2 but not for cytoskeletal organization. *J. Biol. Chem.* 271:14814–14818. doi:10.1074/jbc.271.25.14814
- Cremer, H., R. Lange, A. Christoph, M. Plomann, G. Vopper, J. Roes, R. Brown, S. Baldwin, P. Kraemer, S. Scheff, et al. 1994. Inactivation of the N-CAM gene in mice results in size reduction of the olfactory bulb and deficits in spatial learning. *Nature.* 367:455–459. doi:10.1038/367455a0
- Dailey, L., D. Ambrosetti, A. Mansukhani, and C. Basilico. 2005. Mechanisms underlying differential responses to FGF signaling. *Cytokine Growth Factor Rev.* 16:233–247. doi:10.1016/j.cytogfr.2005.01.007
- Di Guglielmo, G.M., C. Le Roy, A.F. Goodfellow, and J.L. Wrana. 2003. Distinct endocytic pathways regulate TGF-beta receptor signalling and turnover. *Nat. Cell Biol.* 5:410–421. doi:10.1038/nbc975
- Diestel, S., D. Schaefer, H. Cremer, and B. Schmitz. 2007. NCAM is ubiquitinated, endocytosed and recycled in neurons. *J. Cell Sci.* 120:4035–4049. doi:10.1242/jcs.019729
- Dikic, I., and S. Giordano. 2003. Negative receptor signalling. *Curr. Opin. Cell Biol.* 15:128–135. doi:10.1016/S0955-0674(03)00004-8
- Eswarakumar, V.P., I. Lax, and J. Schlessinger. 2005. Cellular signaling by fibroblast growth factor receptors. *Cytokine Growth Factor Rev.* 16:139–149. doi:10.1016/j.cytogfr.2005.01.001
- Fabbri, M., L. Fumagalli, G. Bossi, E. Bianchi, J.R. Bender, and R. Pardi. 1999. A tyrosine-based sorting signal in the beta2 integrin cytoplasmic domain mediates its recycling to the plasma membrane and is required for ligand-supported migration. *EMBO J.* 18:4915–4925. doi:10.1093/emboj/18.18.4915

- Francavilla, C., S. Loeffler, D. Piccini, A. Kren, G. Christofori, and U. Cavallaro. 2007. Neural cell adhesion molecule regulates the cellular response to fibroblast growth factor. *J. Cell Sci.* 120:4388–4394. doi:10.1242/jcs.010744
- Furdui, C.M., E.D. Lew, J. Schlessinger, and K.S. Anderson. 2006. Autophosphorylation of FGFR1 kinase is mediated by a sequential and precisely ordered reaction. *Mol. Cell.* 21:711–717. doi:10.1016/j.molcel.2006.01.022
- Hansen, S.M., S. Li, E. Bock, and V. Berezin. 2008. Synthetic NCAM-derived ligands of the fibroblast growth factor receptor. *Neurochem. Res.* doi: 10.1007/s11064-008-9707-8.
- Haugsten, E.M., V. Sørensen, A. Brech, S. Olsnes, and J. Wesche. 2005. Different intracellular trafficking of FGFR1 endocytosed by the four homologous FGF receptors. *J. Cell Sci.* 118:3869–3881. doi:10.1242/jcs.02509
- Haugsten, E.M., J. Malecki, S.M. Bjorklund, S. Olsnes, and J. Wesche. 2008. Ubiquitination of fibroblast growth factor receptor 1 is required for its intracellular sorting but not for its endocytosis. *Mol. Biol. Cell.* 19:3390–3403. doi:10.1091/mbc.E07-12-1219
- Hinsby, A.M., V. Berezin, and E. Bock. 2004. Molecular mechanisms of NCAM function. *Front. Biosci.* 9:2227–2244. doi:10.2741/1393
- Hoeller, D., S. Volarevic, and I. Dikic. 2005. Compartmentalization of growth factor receptor signalling. *Curr. Opin. Cell Biol.* 17:107–111. doi:10.1016/j.ccb.2005.01.001
- Hopkins, C.R. 1983. Intracellular routing of transferrin and transferrin receptors in epidermoid carcinoma A431 cells. *Cell.* 35:321–330. doi:10.1016/0092-8674(83)90235-0
- Itoh, N., and D.M. Ornitz. 2004. Evolution of the Fgf and Fgfr gene families. *Trends Genet.* 20:563–569. doi:10.1016/j.tig.2004.08.007
- Jékely, G., H.H. Sung, C.M. Luque, and P. Rørth. 2005. Regulators of endocytosis maintain localized receptor tyrosine kinase signaling in guided migration. *Dev. Cell.* 9:197–207. doi:10.1016/j.devcel.2005.06.004
- Jones, M.C., P.T. Caswell, and J.C. Norman. 2006. Endocytic recycling pathways: emerging regulators of cell migration. *Curr. Opin. Cell Biol.* 18:549–557. doi:10.1016/j.ccb.2006.08.003
- Kiryushko, D., I. Korshunova, V. Berezin, and E. Bock. 2006. Neural cell adhesion molecule induces intracellular signaling via multiple mechanisms of Ca<sup>2+</sup> homeostasis. *Mol. Biol. Cell.* 17:2278–2286. doi:10.1091/mbc.E05-10-0987
- Kiselyov, V.V., G. Skladchikova, A.M. Hinsby, P.H. Jensen, N. Kulahin, V. Soroka, N. Pedersen, V. Tsetlin, F.M. Poulsen, V. Berezin, and E. Bock. 2003. Structural basis for a direct interaction between FGFR1 and NCAM and evidence for a regulatory role of ATP. *Structure.* 11:691–701. doi:10.1016/S0969-2126(03)00096-0
- Kiselyov, V.V., V. Soroka, V. Berezin, and E. Bock. 2005. Structural biology of NCAM homophilic binding and activation of FGFR. *J. Neurochem.* 94:1169–1179. doi:10.1111/j.1471-4159.2005.03284.x
- Kos, F.J., and C.S. Chin. 2002. Costimulation of T cell receptor-triggered IL-2 production by Jurkat T cells via fibroblast growth factor receptor 1 upon its engagement by CD56. *Immunol. Cell Biol.* 80:364–369. doi:10.1046/j.1440-1711.2002.01098.x
- Lampugnani, M.G., F. Orsenigo, M.C. Gagliani, C. Tacchetti, and E. Dejana. 2006. Vascular endothelial cadherin controls VEGFR-2 internalization and signaling from intracellular compartments. *J. Cell Biol.* 174:593–604. doi:10.1083/jcb.200602080
- Lehembre, F., M. Yilmaz, A. Wicki, T. Schomber, K. Strittmatter, D. Ziegler, A. Kren, P. Went, P.W. Derksen, A. Berns, et al. 2008. NCAM-induced focal adhesion assembly: a functional switch upon loss of E-cadherin. *EMBO J.* 27:2603–2615. doi:10.1038/emboj.2008.178
- Maness, P.F., and M. Schachner. 2007. Neural recognition molecules of the immunoglobulin superfamily: signaling transducers of axon guidance and neuronal migration. *Nat. Neurosci.* 10:19–26. doi:10.1038/nn1827
- Marmor, M.D., and Y. Yarden. 2004. Role of protein ubiquitylation in regulating endocytosis of receptor tyrosine kinases. *Oncogene.* 23:2057–2070. doi:10.1038/sj.onc.1207390
- Martínez-Arca, S., J.J. Bech-Serra, M. Hurtado-Küttner, A. Borroto, and J. Arribas. 2005. Recycling of cell surface pro-transforming growth factor- $\alpha$  regulates epidermal growth factor receptor activation. *J. Biol. Chem.* 280:36970–36977. doi:10.1074/jbc.M504425200
- Mitchell, H., A. Choudhury, R.E. Pagano, and E.B. Leof. 2004. Ligand-dependent and -independent transforming growth factor- $\beta$  receptor recycling regulated by clathrin-mediated endocytosis and Rab11. *Mol. Biol. Cell.* 15:4166–4178. doi:10.1091/mbc.E04-03-0245
- Mitra, S.K., and D.D. Schlaepfer. 2006. Integrin-regulated FAK-Src signaling in normal and cancer cells. *Curr. Opin. Cell Biol.* 18:516–523. doi:10.1016/j.ccb.2006.08.011
- Mu, F.T., J.M. Callaghan, O. Steele-Mortimer, H. Stenmark, R.G. Parton, P.L. Campbell, J. McCluskey, J.P. Yeo, E.P. Tock, and B.H. Toh. 1995. EEA1, an early endosome-associated protein. EEA1 is a conserved alpha-helical peripheral membrane protein flanked by cysteine “fingers” and contains a calmodulin-binding IQ motif. *J. Biol. Chem.* 270:13503–13511. doi:10.1074/jbc.270.22.13503
- Nielsen, J., N. Kulahin, and P.S. Walmod. 2008. Extracellular protein interactions mediated by the neural cell adhesion molecule, NCAM: heterophilic interactions between NCAM and cell adhesion molecules, extracellular matrix proteins, and viruses. *Neurochem. Res.* doi: 10.1007/s11064-008-9761-2.
- Palamidessi, A., E. Frittoli, M. Garré, M. Faretta, M. Mione, I. Testa, A. Diaspro, L. Lanzetti, G. Scita, and P.P. Di Fiore. 2008. Endocytic trafficking of Rac is required for the spatial restriction of signaling in cell migration. *Cell.* 134:135–147. doi:10.1016/j.cell.2008.05.034
- Palmieri, D., A. Bouadis, R. Ronchetti, M.J. Merino, and P.S. Steeg. 2006. Rab11a differentially modulates epidermal growth factor-induced proliferation and motility in immortal breast cells. *Breast Cancer Res. Treat.* 100:127–137. doi:10.1007/s10549-006-9244-6
- Penengo, L., M. Mapelli, A.G. Murachelli, S. Confalonieri, L. Magri, A. Musacchio, P.P. Di Fiore, S. Polo, and T.R. Schneider. 2006. Crystal structure of the ubiquitin binding domains of rabex-5 reveals two modes of interaction with ubiquitin. *Cell.* 124:1183–1195. doi:10.1016/j.cell.2006.02.020
- Polanska, U.M., D.G. Fernig, and T. Kinnunen. 2009. Extracellular interactome of the FGF receptor-ligand system: complexities and the relative simplicity of the worm. *Dev. Dyn.* 238:277–293. doi:10.1002/dvdy.21757
- Prekeris, R. 2003. Rabs, Rips, FIPs, and endocytic membrane traffic. *ScientificWorldJournal.* 3:870–880. doi:10.1100/tsw.2003.69
- Rabinowitz, J.E., U. Rutishauser, and T. Magnuson. 1996. Targeted mutation of Ncam to produce a secreted molecule results in a dominant embryonic lethality. *Proc. Natl. Acad. Sci. USA.* 93:6421–6424. doi:10.1073/pnas.93.13.6421
- Ren, M., G. Xu, J. Zeng, C. De Lemos-Chiarandini, M. Adesnik, and D.D. Sabatini. 1998. Hydrolysis of GTP on rab11 is required for the direct delivery of transferrin from the pericentriolar recycling compartment to the cell surface but not from sorting endosomes. *Proc. Natl. Acad. Sci. USA.* 95:6187–6192. doi:10.1073/pnas.95.11.6187
- Saffell, J.L., E.J. Williams, I.J. Mason, F.S. Walsh, and P. Doherty. 1997. Expression of a dominant negative FGF receptor inhibits axonal growth and FGF receptor phosphorylation stimulated by CAMs. *Neuron.* 18:231–242. doi:10.1016/S0896-6273(00)80264-0
- Sanchez-Heras, E., F.V. Howell, G. Williams, and P. Doherty. 2006. The fibroblast growth factor receptor acid box is essential for interactions with N-cadherin and all of the major isoforms of neural cell adhesion molecule. *J. Biol. Chem.* 281:35208–35216. doi:10.1074/jbc.M608655200
- Sandilands, E., S. Akbarzadeh, A. Vecchione, D.G. McEwan, M.C. Frame, and J.K. Heath. 2007. Src kinase modulates the activation, transport and signalling dynamics of fibroblast growth factor receptors. *EMBO Rep.* 8:1162–1169. doi:10.1038/sj.embor.7401097
- Secher, T. 2008. Soluble NCAM. *Neurochem. Res.* doi: 10.1007/s11064-008-9743-4.
- Skaper, S.D., W.J. Kee, L. Facci, G. Macdonald, P. Doherty, and F.S. Walsh. 2000. The FGFR1 inhibitor PD 173074 selectively and potently antagonizes FGF-2 neurotrophic and neurotropic effects. *J. Neurochem.* 75:1520–1527. doi:10.1046/j.1471-4159.2000.0751520.x
- Suyama, K., I. Shapiro, M. Guttman, and R.B. Hazan. 2002. A signaling pathway leading to metastasis is controlled by N-cadherin and the FGF receptor. *Cancer Cell.* 2:301–314. doi:10.1016/S1535-6108(02)00150-2
- Walker, J.L., A.K. Fournier, and R.K. Assoian. 2005. Regulation of growth factor signaling and cell cycle progression by cell adhesion and adhesion-dependent changes in cellular tension. *Cytokine Growth Factor Rev.* 16:395–405. doi:10.1016/j.cytogfr.2005.03.003
- Werner, S., W. Weinberg, X. Liao, K.G. Peters, M. Blessing, S.H. Yuspa, R.L. Weiner, and L.T. Williams. 1993. Targeted expression of a dominant-negative FGF receptor mutant in the epidermis of transgenic mice reveals a role of FGF in keratinocyte organization and differentiation. *EMBO J.* 12:2635–2643.
- White, D.P., P.T. Caswell, and J.C. Norman. 2007.  $\alpha$ v $\beta$ 3 and  $\alpha$ 5 $\beta$ 1 integrin recycling pathways dictate downstream Rho kinase signaling to regulate persistent cell migration. *J. Cell Biol.* 177:515–525. doi:10.1083/jcb.200609004
- Williams, E.J., J. Furness, F.S. Walsh, and P. Doherty. 1994. Activation of the FGF receptor underlies neurite outgrowth stimulated by L1, N-CAM, and N-cadherin. *Neuron.* 13:583–594. doi:10.1016/0896-6273(94)90027-2
- Wong, A., B. Lamothe, A. Lee, J. Schlessinger, I. Lax, and A. Li. 2002. FRS2  $\alpha$  attenuates FGF receptor signaling by Grb2-mediated recruitment of the ubiquitin ligase Cbl. *Proc. Natl. Acad. Sci. USA.* 99:6684–6689. doi:10.1073/pnas.052138899
- Xian, W., K.L. Schwertfeger, and J.M. Rosen. 2007. Distinct roles of fibroblast growth factor receptor 1 and 2 in regulating cell survival and

epithelial-mesenchymal transition. *Mol. Endocrinol.* 21:987–1000.  
doi:10.1210/me.2006-0518

Yayon, A., M. Klagsbrun, J.D. Esko, P. Leder, and D.M. Ornitz. 1991. Cell surface, heparin-like molecules are required for binding of basic fibroblast growth factor to its high affinity receptor. *Cell.* 64:841–848.  
doi:10.1016/0092-8674(91)90512-W

Zecchini, S., and U. Cavallaro. 2008. Neural cell adhesion molecule in cancer: expression and mechanisms. *Neurochem. Res.* doi: 10.1007/s11064-008-9597-9.

Zhang, Z., C. Coomans, and G. David. 2001. Membrane heparan sulfate proteoglycan-supported FGF2-FGFR1 signaling: evidence in support of the “cooperative end structures” model. *J. Biol. Chem.* 276:41921–41929.  
doi:10.1074/jbc.M106608200